RF and Microwave Power Amplifier and Transmitter Technologies — *Part 1*

By Frederick H. Raab, Peter Asbeck, Steve Cripps, Peter B. Kenington, Zoya B. Popovic, Nick Pothecary, John F. Sevic and Nathan O. Sokal

With this issue, we begin a four-part series of articles that offer a comprehensive overview of power amplifier technologies. Part 1 covers the key topics of amplifier linearity, efficiency and available RF power devices

RF and microwave power amplifiers and transmitters are used in a wide variety of applications including wireless communication, jamming, imaging, radar, and RF heating. This article provides an introduction and historical background for the subject, and begins the technical discussion with material on signals, linearity, efficiency, and RF-power devices. At the end, there is a convenient summary of the acronyms used—this will be provided with all four installments. Author affiliations and contact information are also provided at the end of each part.

1. INTRODUCTION

The generation of significant power at RF and microwave frequencies is required not only in wireless communications, but also in applications such as jamming, imaging, RF heating, and miniature DC/DC converters. Each application has its own unique requirements for frequency, bandwidth, load, power, efficiency, linearity, and cost. RF power can be generated by a wide variety of techniques using a wide variety of devices. The basic techniques for RF power amplification via classes A, B, C, D, E, and F are reviewed and illustrated by examples from HF through Ka band. Power amplifiers can be combined into transmitters in a similarly wide variety of architectures, including linear, Kahn, envelope tracking, outphasing, and Doherty. Linearity can be improved through techniques such as feedback, feedforward, and predistortion. Also discussed are some recent developments that may find use in the near future.

A power amplifier (PA) is a circuit for converting DC input power into a significant amount of RF/microwave output power. In most cases, a PA is not just a small-signal amplifier driven into saturation. There exists a great variety of different power amplifiers, and most employ techniques beyond simple linear amplification.

A transmitter contains one or more power amplifiers, as well as ancillary circuits such as signal generators, frequency converters, modulators, signal processors, linearizers, and power supplies. The classic architecture employs progressively larger PAs to boost a low-level signal to the desired output power. However, a wide variety of different architectures in essence disassemble and then reassemble the signal to permit amplification with higher efficiency and linearity.

Modern applications are highly varied. Frequencies from VLF through millimeter wave are used for communication, navigation, and broadcasting. Output powers vary from 10 mW in short-range unlicensed wireless systems to 1 MW in long-range broadcast transmitters. Almost every conceivable type of modulation is being used in one system or another. PAs and transmitters also find use in systems such as radar, RF heating, plasmas, laser drivers, magnetic-resonance imaging, and miniature DC/DC converters.

This series of articles is an expanded version of the paper, “Power Amplifiers and Transmitters for RF and Microwave” by the same authors, which appeared in the the 50th anniversary issue of the *IEEE Transactions on Microwave Theory and Techniques*, March 2002. © 2002 IEEE. Reprinted with permission.

No single technique for power amplification nor any single transmitter architecture is best for all applications. Many of the basic techniques that are now coming into use were devised decades ago, but have only recently been made practical because of advances in RF-power devices and supporting circuitry such as digital signal processing (DSP).

2. HISTORICAL DEVELOPMENT

The development of RF power amplifiers and transmitters can be divided into four eras:

Spark, Arc, and Alternator

In the early days of wireless communication (from 1895 to the mid 1920s), RF power was generated by spark, arc, and alternator techniques. The original RF-power device, the spark gap, charges a capacitor to a high voltage, usually from the AC mains. A discharge (spark) through the gap then rings the capacitor, tuning inductor, and antenna, causing radiation of a damped sinusoid. Spark-gap transmitters were relatively inexpensive and capable of generating 500 W to 5 kW from LF to MF [1].

The arc transmitter, largely attributed to Poulsen, was a contemporary of the spark transmitter. The arc exhibits a negative-resistance characteristic which allows it to operate as a CW oscillator (with some fuzziness). The arc is actually extinguished and reignited once per RF cycle, aided by a magnetic field and hydrogen ions from alcohol dripped into the arc chamber. Arc transmitters were capable of generating as much as 1 MW at LF [2].

The alternator is basically an AC generator with a large number of poles. Early RF alternators by Tesla and Fessenden were capable of operation at LF, and a technique developed by Alexanderson extended the operation to LF [3]. The frequency was controlled by adjusting the rotation speed and up to 200 kW could be generated by a single alternator. One such transmitter (SAQ) remains operable at Grimeton, Sweden.

Vacuum Tubes

With the advent of the DeForest audion in 1907, the thermoionic vacuum tube offered a means of electronically generating and controlling RF signals. Tubes such as the RCA UV-204 (1920) allowed the transmission of pure CW signals and facilitated the transition to higher frequencies of operation.

Younger readers may find it convenient to think of a vacuum tube as a glass-encapsulated high-voltage FET with heater. Many of the concepts for modern electronics, including class-A, -B, and -C power amplifiers, originated early in the vacuum-tube era. PAs of this era were characterized by operation from high voltages into high-impedance loads and by tuned output networks. The basic circuits remained relatively unchanged throughout most of the era.

Vacuum tube transmitters were dominant from the late 1920s through the mid 1970s. They remain in use today in some high power applications, where they offer a relatively inexpensive and rugged means of generating 10 kW or more of RF power.

Discrete Transistors

Discrete solid state RF-power devices began to appear at the end of the 1960s with the introduction of silicon bipolar transistors such as the 2N6093 (75 W HF SSB) by RCA. Power MOSFETs for HF and VHF appeared in 1974 with the VMP-4 by Siliconix. GaAs MESFETs introduced in the late 1970s offered solid state power at the lower microwave frequencies.

The introduction of solid-state RF-power devices brought the use of lower voltages, higher currents, and relatively low load resistances. Ferrite-loaded transmission line transformers enabled HF and VHF PAs to operate over two decades of bandwidth without tuning. Because solid-state devices are temperature-sensitive, bias stabilization circuits were developed for linear PAs. It also became possible to implement a variety of feedback and control techniques through the variety of op-amps and ICs.

Solid-state RF-power devices were offered in packaged or chip form. A single package might include a number of small devices. Power outputs as high as 600 W were available from a single packaged push-pull device (MRF157). The designer basically selected the packaged device that best fit the requirements. How the transistors were made was regarded as a bit of sorcery that occurred in the semiconductor houses and was not a great concern to the ordinary circuit designer.

Custom/Integrated Transistors

The late 1980s and 1990s saw a proliferation variety of new solid-state devices including HEMT, pHEMT, HFET, and HBT, using a variety of new materials such as InP, SiC, and GaN, and offering amplification at frequencies to 100 GHz or more. Many such devices can be operated only from relatively low voltages. However, many current applications need only relatively low power. The combination of digital signal processing and microprocessor control allows widespread use of complicated feedback and predistortion techniques to improve efficiency and linearity.

Many of the newer RF-power devices are available only on a made-to-order basis. Basically, the designer selects a semiconductor process and then specifies the size (e.g., gate periphery). This facilitates tailoring the device to a specific power level, as well as incorporating it into an RFIC or MMIC.

3. LINEARITY

The need for linearity is one of the principal drivers in the design of

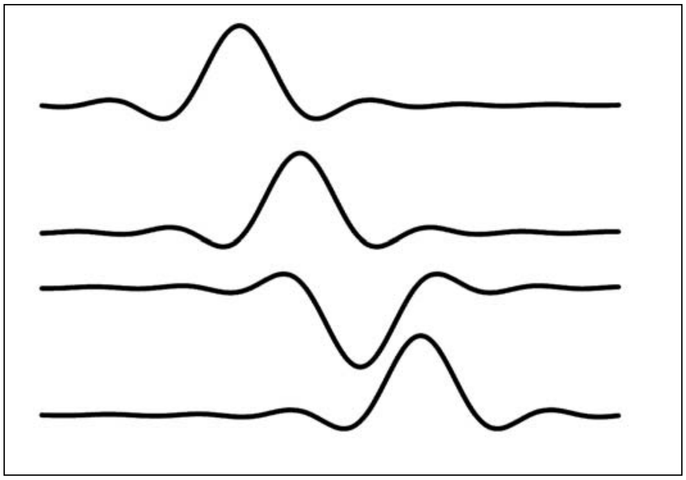

Figure 1 · SRRC data pulses.

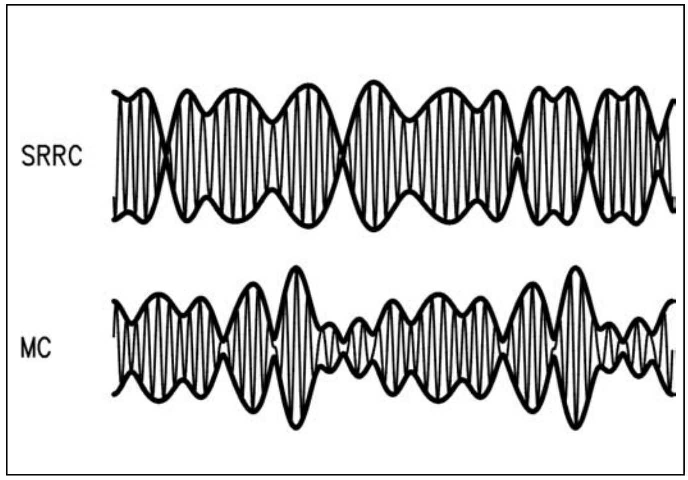

Figure 2 · RF waveforms for SRRC and multicarrier signals.

modern power amplifiers. Linear amplification is required when the signal contains both amplitude and phase modulation. It can be accomplished either by a chain of linear PAs or a combination of nonlinear PAs. Nonlinearities distort the signal being amplified, resulting in splatter into adjacent channels and errors in detection.

Signals such as CW, FM, classical FSK, and GMSK (used in GSM) have constant envelopes (amplitudes) and therefore do not require linear amplification. Full-carrier amplitude modulation is best produced by high level amplitude modulation of the final RF PA. Classic signals that require linear amplification include single sideband (SSB) and vestigal-sideband (NTSC) television. Modern signals that require linear amplification include shaped-pulse data modulation and multiple carriers.

Shaped Data Pulses

Classic FSK and PSK use abrupt frequency or phase transitions, or equivalently rectangular data pulses. The resultant RF signals have constant amplitude and can therefore be amplified by nonlinear PAs with good efficiency. However, the resultant sinc-function spectrum spreads signal energy over a fairly wide bandwidth. This was satisfactory for relatively low data rates and a relatively uncrowded spectrum.

Modern digital signals such as QPSK or QAM are typically generated by modulating both I and Q subcarriers. The requirements for both high data rates and efficient utilization of the increasingly crowded spectrum necessitates the use of shaped data pulses. The most widely used method is based upon a raised-cosine channel spectrum, which has zero intersymbol interference during detection and can be made arbitrarily close to rectangular [4]. A raised-cosine channel spectrum is achieved by using a square-root raised-cosine (SRRC) filter in both the transmitter and receiver. The resultant SRRC data pulses (Figure 1) are shaped somewhat like sinc functions which are truncated after several cycles. At any given time, several different data pulses contribute to the I and Q modulation waveforms. The resultant modulated carrier (Figure 2) has simultaneous amplitude and phase modulation with a peak-to-average ratio of 3 to 6 dB.

Multiple Carriers and OFDM

Applications such as cellular base stations, satellite repeaters, and multi-beam “active-phased-array” transmitters require the simultaneous amplification of multiple signals. Depending on the application, the signals can have different amplitudes, different modulations, and irregular frequency spacing.

In a number of applications including HF modems, digital audio broadcasting, and high-definition television, it is more convenient to use a large number of carriers with low data rates than a single carrier with a high data rate. The motivations include simplification of the modulation/demodulation hardware, equalization, and dealing with multipath propagation. Such Orthogonal Frequency Division Multiplex (OFDM) techniques [5] employ carriers with the same amplitude and modulation, separated in frequency so that modulation products from one carrier are zero at the frequencies of the other carriers.

Regardless of the characteristics of the individual carriers, the resultant composite signal (Figure 2) has simultaneous amplitude and phase modulation. The peak-to-average ratio is typically in the range of 8 to 13 dB.

Nonlinearity

Nonlinearities cause imperfect reproduction of the amplified signal, resulting in distortion and splatter. Amplitude nonlinearity causes the instantaneous output amplitude or

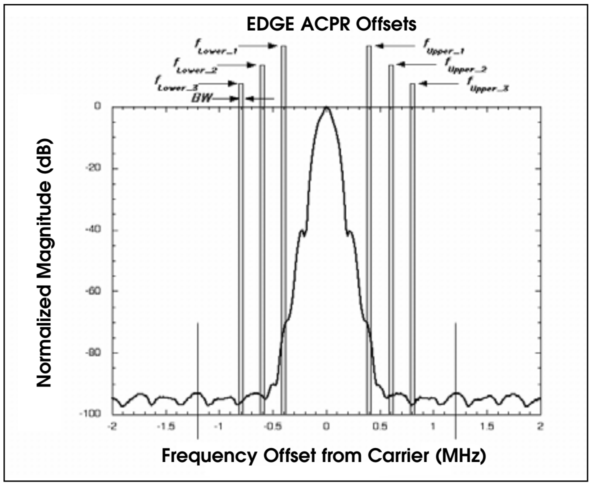

Figure 3 · ACPR offsets and bandwidths.

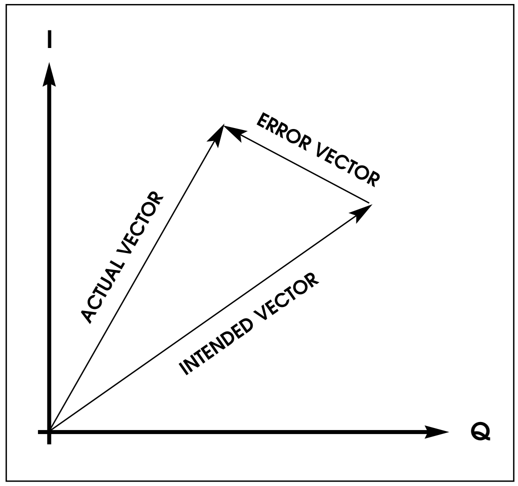

Figure 4 · Error vector.

envelope to differ in shape from the corresponding input. Such nonlinearities are the variable gain or saturation in a transistor or amplifier. Amplitude-to-phase conversion is a phase shift associated with the signal amplitude and causes the introduction of unwanted phase modulation into the output signal. Amplitude-to-phase conversion is often associated with voltage-dependent capacitances in the transistors. While imperfect frequency response also distorts a signal, it is a linear process and therefore does not generate out-of-band signals.

Amplitude nonlinearity and amplitude-to-phase conversion are described by transfer functions that act upon the instantaneous signal voltage or envelope. However, memory effects can also occur in high-power PAs because of thermal effects and charge storage. Thermal effects are somewhat more noticeable in III-V semiconductors because of lower thermal conductivity, while charge-storage effects are more prevalent in overdriven BJT PAs.

Measurement of Linearity

Linearity is characterized, measured, and specified by various techniques depending upon the specific signal and application. The linearity of RF PAs is typically characterized by C/I, NPR, ACPR, and EVM (defined below).

STANDARD	Offset 1	Offset 2	BW (kHz)	Integration Filter	EVM (peak/rms)
NADC [13]	±30 kHz –26 dBc	±60 kHz –45 dBc	32.8 kHz	RRC α=0.35	25%/12%
PHS [14]	±600 kHz –50 dBc	±900 kHz –55 dBc	37.5 kHz	RRC α=0.50	25%/12%
EDGE [15]	±400 kHz –58 dBc	±600 kHz –66 dBc	30 kHz	None	22%/7.0%
TETRA [16]	25 kHz –60 dBc	50 kHz –70 dBc	25 kHz	RRC α=0.35	30%/10%
IS-95 CDMA [17]	885 kHz –45 dBc	1980 kHz –55 dBc	30 kHz	None	N/A
W-CDMA (3G-PP) [18]	5.00 MHz –33 dB	10.0 MHz –43 dB	4.68 MHz	RRC α=0.22	25%/N/A

Table 1 · ACPR and EVM requirements of various systems.

The traditional measure of linearity is the carrier-to-intermodulation (C/I) ratio. The PA is driven with two or more carriers (tones) of equal amplitudes. Nonlinearities cause the production of intermodulation products at frequencies corresponding to sums and differences of multiples of the carrier frequencies [6]. The amplitude of the third-order or maximum intermodulation distortion (IMD) product is compared to that of the carriers to obtain the C/I. A typical linear PA has a C/I of 30 dB or better.

Noise-Power Ratio (NPR) is a traditional method of measuring the linearity of PAs for broadband and noise-like signals. The PA is driven with Gaussian noise with a notch in one segment of its spectrum. Nonlinearities cause power to appear in the notch. NPR is the ratio of the notch power to the total signal power.

Adjacent Channel Power Ratio (ACPR) characterizes how nonlinearity affects adjacent channels and is widely used with modern shaped-pulse digital signals such as NADC and CDMA. Basically, ACPR is the ratio of the power in a specified band outside the signal bandwidth to the rms power in the signal (Figure 3). In some cases, the actual power spectrum $S(f)$ is weighted by the frequency response $H(f)$ of the pulse-shaping filter; i.e. (eq. 1)

$$ACPR_{lower} = \frac{\int_{f_c-f_o-BW/2}^{f_c-f_o+BW/2} \left|H(f)\right|^2 S(f)df}{\int_{f_L}^{f_U} \left|H(f)\right|^2 S(f)df}$$

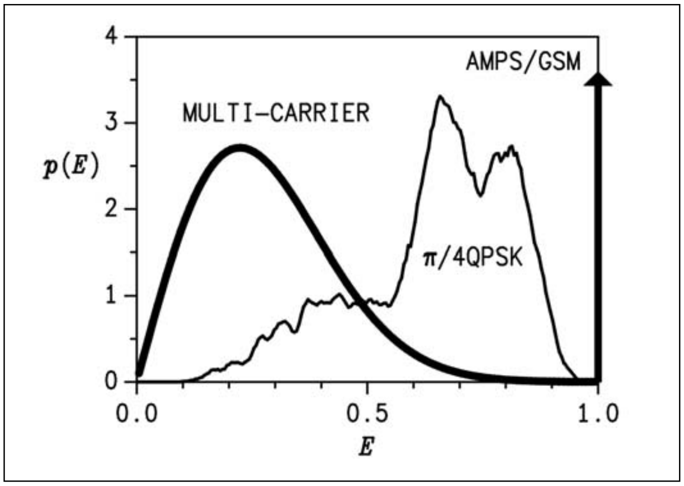

Figure 5 · Envelope PDFs.

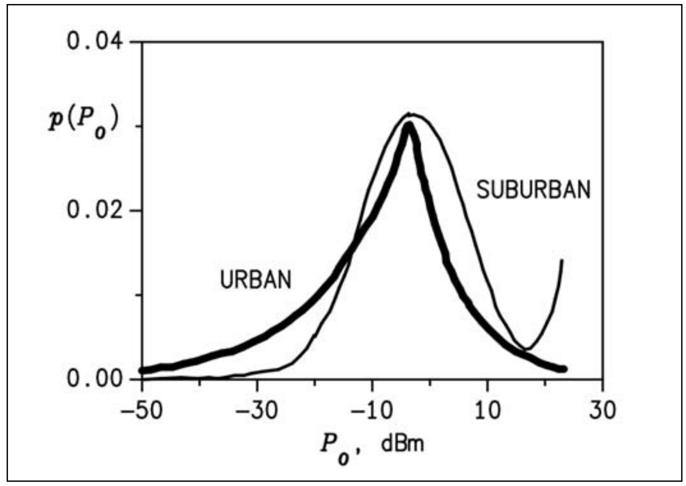

Figure 6 · Power-output PDFs.

where f_c is the center frequency, B is the bandwidth, f_o is the offset, and f_L and f_U are the band edges. The weighting, frequency offsets, and required ACPRs vary with application as shown in Table 1. ACPR can be specified for either upper or lower sideband. In many cases, two different ACPRs for two different frequency offsets are specified. ACPR2, based upon the outer band, is sometimes called "Alternate Channel Power Ratio."

Error Vector Magnitude (EVM) is a convenient measure of how nonlinearity interferes with the detection process. EVM is defined (Figure 4) as the distance between the desired and actual signal vectors, normalized to a fraction of the signal amplitude. Often, both peak and rms errors are specified (Table 1).

4. EFFICIENCY

Efficiency, like linearity, is a critical factor in PA design. Three definitions of efficiency are commonly used. Drain efficiency is defined as the ratio of RF output power to DC input power:

$$\eta = P_{out}/P_{in} \tag{2}$$

Power-added efficiency (PAE) incorporates the RF drive power by subtracting it from the output power; i.e. $(P_{out} - P_{DR})/P_{in}$. PAE gives a reasonable indication of PA performance when gain is high; however, it can become negative for low gains. An overall efficiency such as $Pout/(P_{in} + P_{DR})$ is useable in all situations. This definition can be varied to include driver DC input power, the power consumed by supporting circuits, and anything else of interest.

Average Efficiency

The instantaneous efficiency is the efficiency at one specific output level. For most PAs, the instantaneous efficiency is highest at the peak output power (PEP) and decreases as output decreases. Signals with time-varying amplitudes (amplitude modulation) therefore produce time-varying efficiencies. A useful measure of performance is then the average efficiency, which is defined [7] as the ratio of the average output power to the average DC-input power:

$$\eta_{AVG} = P_{outAVG}/P_{inAVG} \tag{3}$$

This concept can be used with any of the three definitions of efficiency.

The probability-density function (PDF) of the envelope gives the relative amount of time an envelope spends at various amplitudes (Figure 5). Also used is the cumulative distribution function (CDF), which gives the probability that the envelope does not exceed a specified amplitude. CW, FM, and GSM signals have constant envelopes and are therefore always at peak output. SRRC data modulation produces PDFs that are concentrated primarily in the upper half of the voltage range and have peak-to-average ratios on the order of 3 to 6 dB. Multiple carriers [8] produce random-phasor sums much like random noise and therefore have Rayleigh-distributed envelopes; i.e.,

$$p(E) = 2\,E\,\xi\exp(-V_2\,\xi) \tag{4}$$

Peak-to-average ratio ξ is typically between 6 and 13 dB.

The average input and output powers are found by integrating the product of their variation with amplitude and the PDF of the envelope. Two cases are of special interest. When the DC input current is constant (class-A bias), the DC input power is also constant. The average efficiency is then η_{PEP}/ξ. If the DC input current (hence power) is proportional to the envelope (as in class-B), the average efficiency is $(4/\pi)^{1/2}$ η_{PEP}, for a Rayleigh-distributed signal. Thus for a multicarrier signal with a 10 dB peak-to-average ratio, ideal class-A and B PAs with PEP efficiencies of 50 and 78.5 percent, respectively, have average efficiencies of only 5 and 28 percent, respectively.

Back-Off

The need to conserve battery power and to avoid interference to other users operating on the same frequency necessitates the transmission of signals whose peak amplitudes well below the peak output power of the transmitter. Since peak power is needed only in the worst-case links, the "back-off" is typically in the range of 10 to 20 dB.

For a single-carrier mobile transmitter, back-off rather than envelope PDF is dominant in determining the average power consumption and average efficiency. The PDF of the transmitting power (Figure 4) depends not only upon the distance, but also upon factors such as attenuation by buildings, multipath, and orientation of the mobile antenna [8], [9], [10]. To facilitate prediction of the power consumption, the envelope and back-off PDFs can be combined [11].

5. RF POWER TRANSISTORS

A wide variety of active devices is currently available for use in RF-power amplifiers, and RF-power transistors are available in packaged, die, and grown-to-order forms. Packaged devices are used at frequencies up to X band, and are dominant for high power and at VHF and lower frequencies. A given package can contain one or more die connected in parallel and can also include internal matching for a specific frequency of operation. Dice (chips) can be wire-bonded directly into a circuit to minimize the effects of the package and are used up to 20 GHz. In MMICs, the RF-power device is grown to order, allowing its size and other characteristics to be optimized for the particular application. This form of construction is essential for upper-microwave and millimeter-wave frequencies to minimize the effects of strays and interconnects. Virtually all RF power transistors are npn or n-channel types because the greater mobility of electrons (vs. holes) results in better operation at higher frequencies.

Bipolar Junction Transistor (BJT)

The Si BJT is the original solid-state RF power device, originating in the 1960s. Since the BJT is a vertical device, obtaining a high collector-breakdown voltage is relatively simple and the power density is very high. Si BJTs typically operate from 28 V supplies and remain in use at frequencies up to 5 GHz, especially in high-power (1 kW) pulsed applications such as radar. While Si RF power devices have higher gain at high frequencies, their fundamental properties are basically those of ordinary bipolar transistors. The positive temperature coefficient of BJTs tends to allow current hogging, hot-spotting, and thermal runaway, necessitating carefully regulated base bias. Since RF power BJTs are generally composed of multiple, small BJTs (emitter sites), emitter ballasting (resistance) is generally employed to force even division of the current within a given package.

Metal-Oxide-Silicon Field-Effect Transistor (MOSFET)

MOSFETs are constructed with insulated gates. Topologies with both vertical and later current flow are used in RF applications, and most are produced by a double-diffusion process. Because the insulated gate conducts no DC current, MOSFETs are very easily biased.

The negative temperature coefficient of a MOSFET causes its drain current to decrease with temperature. This prevents thermal runaway and allows multiple MOSFETs to be connected in parallel without ballasting. The absence of base-charge storage time allows fast switching and also eliminates a mechanism for subharmonic oscillation. An overdriven (saturated) MOSFET can conduct drain current in either direction, which is very useful in switching-mode operation with reactive loads.

Vertical RF power MOSFETs are useable through VHF and UHF. Gemini-packaged devices can deliver up to 1 kW at HF and 100s of watts at VHF. VMOS devices typically operate from 12, 28, or 50-V supplies, although some devices are capable of operation from 100 V or more.

Laterally Diffused MOS (LDMOS)

LDMOS is especially useful at UHF and lower microwave frequencies because direct grounding of its source eliminates bond-wire inductance that produces negative feedback and reduces gain at high frequencies. This also eliminates the need for the BeO insulating layer commonly used in other RF-power MOSFETs.

LDMOS devices typically operate from 28-V supplies and are currently available with power outputs of 120 W at 2 GHz. They are relatively low in cost compared to other devices for this frequency range and are currently the device of choice for use in high-power transmitters at 900 MHz and 2 GHz.

Junction FET (JFET)

JFETs for power applications are often called Static Induction Transistors (SITs). Impressive power and efficiency have been obtained from RF JFETs based upon Si, SiGe, and SiC at frequencies through UHF. However, the JFET has never become as popular as other RF-power FETs.

GaAs MEtal Semiconductor FET (GaAs MESFET)

GaAs MESFETs are JFETs based upon GaAs and a Schottky gate junction. They have higher mobility than do Si devices and are therefore capable of operating efficiently at higher frequencies. GaAs MESFETs are widely used for the production of microwave power, with capabilities of up 200 W at 2 GHz and 40 W at 20 GHz in packaged devices. These devices have relatively low breakdown voltages compared to MOSFETs or JFETs and are typically operated from supply voltages (drain biases) of 5 to 10 V. Most MESFETs are depletion-mode devices and require a negative gate bias, although some enhance-mode devices that operate with a positive bias have been developed. Linearity is often poor due to input capacitance variation with voltage; the output capacitance is also often strongly bias- and frequency-dependent.

Heterojunction FET (HFET) / High-Electron-Mobility Transistor (HEMT)

HFETs and HEMTs improve upon the MESFET geometry by separating the Schottky and channel functions. Added to the basic MESFET structure is a heterojunction consisting of an n-doped AlGaAs Schottky layer, an undoped AlGaAs spacer, and an undoped GaAs channel. The discontinuity in the band gaps of AlGaAs and GaAs causes a thin layer of electrons ("two-dimensional electron gas or 2-DEG") to form below the gate at the interface of the AlGaAs and GaAs layers. Separation of the donors from the mobile electrons reduces collisions in the channel, improving the mobility, and hence high-frequency response, by a factor of about two.

AlGaAs has crystal-lattice properties similar to those of GaAs, and this makes it possible to produce a potential difference without lattice stress. The GaAs buffer contributes to a relatively high breakdown voltage. Their fabrication employs advanced epitaxial technologies (Molecular Beam Epitaxy or Metal Organic Chemical Vapor Deposition) which tends to increase their cost.

The GaAs HEMT is known in the literature by a wide variety of different names, including MODFET (Modulation-Doped FET), TEGFET (Two-dimensional Electron-Gas FET), and SDFET (Selectively Doped FET). It is also commonly called an HFET (Heterostructure FET), although technically an "HFET" has a doped channel that provides the carriers (instead of the heterojunction). The acronyms "HFET and "HJFET" (HeteroJunction FET) appear to be used interchangeably.

GaAs HEMTs/HFETs with f_T as high as 158 GHz are reported. PAs based upon these HEMTs exhibit 15-W outputs at 12 GHz with a power-added efficiency (PAE) of 50 percent. Outputs of 100 W are available at S band from packaged devices.

Pseudomorphic HEMT

The pseudomorphic HEMT (pHEMT) further improves upon the basic HEMT by employing an InGaAs channel. The increased mobility of In with respect to GaAs increases the bandgap discontinuity and therefore the number of carriers in the two-dimensional electron gas. The lattice mismatch between the GaInAs channel and GaAs substrate is also increased, however, and this limits the In content to about 22 percent.

The efficiency of PAs using pHEMTs does not begin to drop until about 45 GHz and pHEMTs are useable to frequencies as high as 80 GHz. Power outputs vary from 40 W at L band to 100 mW at V band. While pHEMTs are normally grown to order, a packaged device pHEMT has recently become available.

InP HEMT

The InP HEMT places an AlInAs/GaInAs heterojunction on an InP substrate. The lattices are more closely matched, which allows an In content of up to about 53 percent. This results in increased mobility, which in turn results in increased electron velocity, increased conduction-band discontinuity, increased two-dimensional electron gas, and higher transconductance. The thermal resistance is 40 percent lower than that of a comparable device built on a GaAs substrate.

The InP HEMT has higher gain and efficiency than the GaAs pHEMT, with the PA efficiency beginning to drop at 60 GHz. However, it has a lower breakdown voltage (typically 7 V) and must therefore be operated from a relatively low drain-voltage supply (e.g., 2 V). This results in lower output per device and possibly loss in the combiners required to achieve a specified output power. Nonetheless, the InP HEMT generally has a factor-of-two efficiency advantage over the pHEMT and GaAs HEMT.

InP HEMTs have been fabricated with fmax as high as 600 GHz (0.1 μm gate length), and amplification has been demonstrated at frequencies as high as 190 GHz. The efficiency does not begin to drop until about 60 GHz. Power levels range from 100 to 500 mW per chip.

Metamorphic HEMT (mHEMT)

The mHEMT allows channels with high-In content to be built on GaAs substrates. The higher electron mobility and higher peak saturation velocity result in higher gain than is possible in a pHEMT. mHEMTs are generally limited to low-power applications by their relatively low breakdown voltage (<3 V). However, an mHEMT capable of 6-V operation and a power output of 0.5 W has been recently reported.

Heterojunction Bipolar Transistor (HBT)

HBTs are typically based upon the compound-semiconductor material AlGaAs/GaAs. The AlGaAs emitter is made as narrow as possible to minimize base resistance. The base is a thin layer of p GaAs. The barrier is created by heterojunction (AlGaAs/GaAs) rather than the doping. The base can therefore be doped heavily to minimize its resistance. Base sheet resistance is typically two orders of magnitude lower than that of an ordinary BJT, and the frequency of operation is accordingly higher. The current flow is (in contrast to a MES-

FET) vertical so that surface imperfections have less effect upon performance. The use of a semi-insulating substrate and the higher electron mobility result in reduced parasitics. The DC curves are somewhat similar to those of a conventional BJT, but often contain a saturation resistance as well as saturation voltage. Currently available AlGaAs/GaAs HBTs are capable of producing several watts and are widely used in wireless handsets, GaAs HBTs are also widely used in MMIC circuits at frequencies up to X band and can operate in PAs at frequencies as high as 20 GHz.

SiGe HBT

The use of SiGe rather than Si in the base of the HBT both increases the maximum operating frequency and decreases the base resistance. However, they are generally less efficient than GaAs HBTs and can have lower breakdown voltages. One experimental SiGe HBT is capable of delivering over 200 W at L band.

InP HBT

The use of InP in an HBT further boosts mobility and therefore the high frequency response. In addition, InP HBTs have lower turn-on and knee voltages, resulting in higher gain and efficiency. InP HBTs for RF-power applications incorporate two heterojunctions (AlInAs/GaInAs and GaInAs/InP). The InP in the collector increases the breakdown voltage, allowing higher output power. To date, outputs of about 0.5 W at 20 GHz have been demonstrated, but it is anticipated that operation to 50 or 60 GHz will be possible.

SiC MESFET

The wide band gap of SiC results in both high mobility and high breakdown voltage. An SiC MESFET can therefore have a frequency response comparable to that of a GaAs MESFET, but breakdown voltages double that of Si LDMOS. This results in power densities of 10 W/mm, which is ten times that of a GaAs MESFET. The high thermal conductivity of the SiC substrate is particularly useful in high-power applications. The higher operating voltage and associated higher load impedance greatly simplify output networks and power combining. SiC MESFETs typically operate from a 48-V supply. Devices with outputs of 10 W are currently available, and outputs of 60 W or more have been demonstrated experimentally. The cost of SiC devices is at presently about ten times that of Si LDMOS.

GaN HEMT

GaN offers the same high breakdown voltage of SiC, but even higher mobility. Its thermal conductivity is, however, lower, hence GaN devices must be built substrate such as SiC or diamond. While the GaN HEMT offers the promise of a high-power, high-voltage device operating at frequencies of 10 GHz or more, it is still in an experimental state. Power outputs of 8 W at 10 GHz with 30 percent efficiency have been demonstrated.

Monolithic Microwave Integrated Circuit (MMIC)

MMICs integrate RF power devices and matching/decoupling elements such as on-chip inductors, capacitors, resistors, and transmission lines. The proximity of these elements to the RF-power devices is essential for input, output, and interstage matching at microwave and millimeter-wave frequencies.

References

1. W. J. Bryon, “Arcs and sparks, Part 1,” *Communications Quarterly*, vol. 4, no. 2, pp. 27-43, Spring 1994.

2. W. J. Bryon, “The arc method of producing continuous waves,” *Communications Quarterly*, vol. 8, no. 3, pp. 47-65, Summer 1998.

3. K. M. MacIlvain and W. H. Freedman, Radio Library, Vol. III: *Radio Transmitters and Carrier Currents*, Scranton PA: International Textbook Company, 1928.

4. J. B. Groe and L. E. Larson, *CDMA Mobile Radio Design,* Norwood, MA: Artech House, 2000.

5. R. van Nee and R. Prasad, *OFDM for Wireless Multimedia Communications*, Norwood, MA: Artech House, 2000.

6. H. L. Krauss, C. W. Bostian, and F. H. Raab, *Solid State Radio Engineering*, New York: Wiley, 1980.

7. F. H. Raab, “Average efficiency of power amplifiers,” *Proc. RF Technology Expo '86*, Anaheim, CA, pp. 474-486, Jan. 30-Feb. 1, 1986.

8. N. Pothecary, “Feedforward linear power amplifiers,” in *Workshop Notes WFB*, Int’l. Microwave Symp., Boston, MA, June 16, 2001.

9. J. F. Sevic, “Statistical characterization of RF power amplifier efficiency for wireless communication systems,” *Proc. Wireless Commun. Conf.*, Boulder, CO, pp. 1-4, Aug. 1997.

10. G. Hanington, P.-F. Chen, P. M. Asbeck, and L. E. Larson, “High-efficiency power amplifier using dynamic power-supply voltage for CDMA applications,” *IEEE Trans. Microwave Theory Tech.*, vol. 47, no. 8, pp. 1471-1476, Aug. 1999.

11. I. Kipnis, “Refining CDMA mobile-phone power control,” *Microwaves & RF*, vol. 39, no. 6, pp. 71-76, June 2000.

12. J. Staudinger, “Applying switched gain stage concepts to improve efficiency and linearity for mobile CDMA power amplification,” *Microwave Journal*, vol. 43, no. 9, pp. 152-162, Sept. 2000.

Table 1 References

13. “Mobile station – base station interoperability standard for dual-mode cellular system,” ANSI-136 Standard, Telecommun. Industries Assoc., 2000.

14. “Digital cellular communication systems,” RCR STD-27, Research and Development Center for Radio Systems (RCR), April 1991.

Acronyms Used in Part 1

AC	Alternating Current
ACPR	Adjacent-Channel Power Ratio
BJT	Bipolar-Junction Transistor
C/I	Carrier-to-Intermodulation
CDF	Cumulative Distribution Function
CDMA	Code-Division Multiple Access
CW	Continuous Wave
DC	Direct Current
DSP	Digital Signal Processing
EVM	Error-Vector Magnitude
FET	Field-Effect Transistor
FSK	Frequency-Shift Keying
GMSK	Gaussian Minimum Shift Keying
GSM	Global System for Mobile communication
HBT	Heterojunction bipolar transistor
HEMT	High Electron-Mobility Transistor
HFET	Heterojunction FET (also HJFET)
IC	Integrated Circuit
JFET	Junction Field-Effect Transistor
LDMOS	Laterally Diffused MOS (FET)
MESFET	MEtal Semiconductor FET
mHEMT	Metamorphic HEMT
MMIC	Microwave Monolithic Integrated Circuit
MOSFET	Metal-Oxide-Silicon Field-Effect Transistor
NADC	North American Digital Cellular
NPR	Noise-Power Ratio
NTSC	National Television Standards Committee
OFDM	Orthogonal Frequency-Division Multiplex
PA	Power Amplifier
PAE	Power-Added Efficiency
PDF	Probability-Density Function
PEP	Peak-Envelope Power
pHEMT	Pseudomorphic HEMT
PSK	Phase-Shift Keying
QAM	Quadrature Amplitude Modulation
QPSK	Quadrature Phase Shift Keying
RF	Radio Frequency
SRRC	Square-Root Raised Cosine
SSB	Single SideBand

15. "Digital cellular telecommunications system (phase 2+), radio transmission and reception," GSM 5.05 Standard, v. 8.4.1, European Telecommun. Standards Inst., 1999.

16. "Terrestrial trunked radio (TETRA) voice+data air interface," TETRA Draft Standard, European Telecommun. Standards Inst., 1999.

17. "Mobile station – base station interoperability standard for dual-mode wideband spread-spectrum cellular system," TIA/EIA IS-95 Interim Standard, Telecommun. Industries Assoc., July 1993.

18. "UE radio transmission and reception (FDD)," TS 25.101, v. 3.4.1, Third Generation Partnership Project, Technical Specification Group, 1999.

Series Notes

1. The remaining three parts of this series will appear in successive issues of *High Frequency Electronics* (July, September and November 2003 issues).

2. To maintain continuity, all figures, tables, equations and references will be numbered sequentially throughout the entire series.

3. Like all articles in *High Frequency Electronics*, this series will be archived and available for downloading (for personal use by individuals only) online at the magazine website: www.highfrequencyelectronics.com

Author Information

The authors of this series of articles are: Frederick H. Raab (lead author), Green Mountain Radio Research, e-mail: f.raab@ieee.org; Peter Asbeck, University of California at San Diego; Steve Cripps, Hywave Associates; Peter B. Kenington, Andrew Corporation; Zoya B. Popovic, University of Colorado; Nick Pothecary, Consultant; John F. Sevic, California Eastern Laboratories; and Nathan O. Sokal, Design Automation. Readers desiring more information should contact the lead author.

From May 2003 *High Frequency Electronics*

RF and Microwave Power Amplifier and Transmitter Technologies — *Part 2*

By Frederick H. Raab, Peter Asbeck, Steve Cripps, Peter B. Kenington, Zoya B. Popovich, Nick Pothecary, John F. Sevic and Nathan O. Sokal

Our multi-part series on power amplifier technologies and applications continues with a review of amplifier configurations, classes of operation, device characterization and example applications

Part 1 of this series introduced basic concepts, discussed the characteristics of signals to be amplified, and gave background information on RF power devices. Part 2 reviews the basic techniques, ratings, and implementation methods for power amplifiers operating at HF through microwave frequencies.

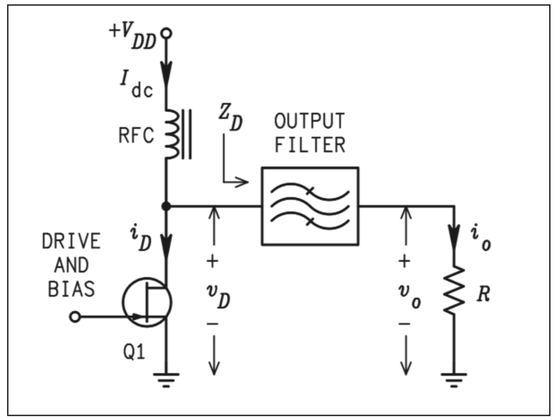

Figure 7 · A single-ended power amplifier.

6a. BASIC TECHNIQUES FOR RF POWER AMPLIFICATION

RF power amplifiers are commonly designated as classes A, B, C, D, E, and F [19]. All but class A employ various nonlinear, switching, and wave-shaping techniques. Classes of operation differ not in only the method of operation and efficiency, but also in their power-output capability. The power-output capability ("transistor utilization factor") is defined as output power per transistor normalized for peak drain voltage and current of 1 V and 1 A, respectively. The basic topologies (Figures 7, 8 and 9) are single-ended, transformer-coupled, and complementary. The drain voltage and current waveforms of selected ideal PAs are shown in Figure 10.

Class A

In class A, the quiescent current is large enough that the transistor remains at all times in the active region and acts as a current source, controlled by the drive. Consequently, the drain voltage and current waveforms are (ideally) both sinusoidal. The power output of an ideal class-A PA is

$$P_o = V_{om}^2 / 2R \qquad (5)$$

where output voltage V_{om} on load R cannot exceed supply voltage V_{DD}. The DC-power input is constant and the efficiency of an ideal PA is 50 percent at PEP. Consequently, the instantaneous efficiency is proportional to the power output and the average efficiency is inversely proportional to the peak-to-average ratio (e.g., 5 percent for x = 10 dB). The utilization factor is 1/8.

For amplification of amplitude-modulated signals, the quiescent current can be varied in proportion to the instantaneous signal envelope. While the efficiency at PEP is unchanged, the efficiency for lower ampli-

This series of articles is an expanded version of the paper, "Power Amplifiers and Transmitters for RF and Microwave" by the same authors, which appeared in the the 50th anniversary issue of the *IEEE Transactions on Microwave Theory and Techniques*, March 2002. © 2002 IEEE. Reprinted with permission.

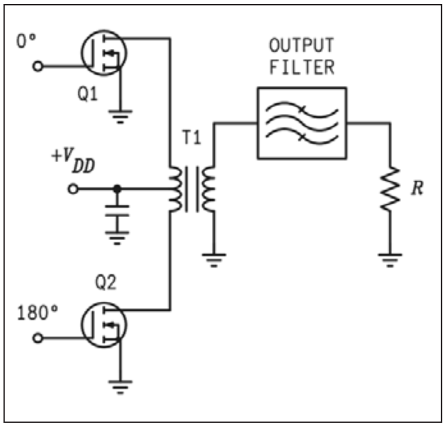

Figure 8 · Transformer-coupled push-pull PA.

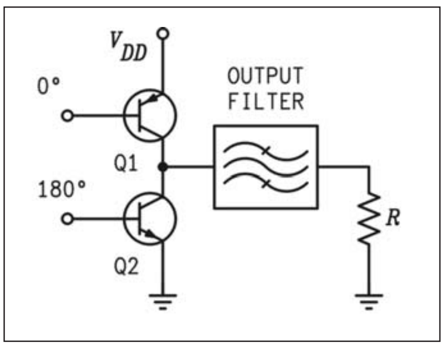

Figure 9 · Complementary PA.

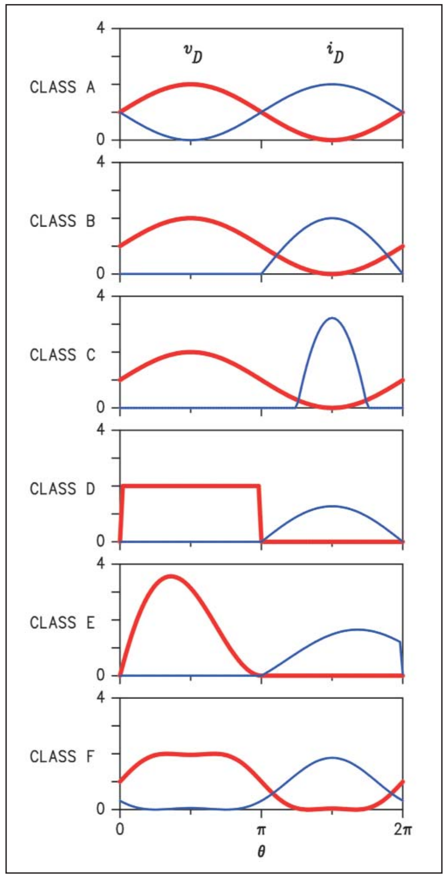

Figure 10 · Wavefroms for ideal PAs.

tudes is considerably improved. In an FET PA, the implementation requires little more than variation of the gate-bias voltage.

The amplification process in class A is inherently linear, hence increasing the quiescent current or decreasing the signal level monotonically decreases IMD and harmonic levels. Since both positive and negative excursions of the drive affect the drain current, it has the highest gain of any PA. The absence of harmonics in the amplification process allows class A to be used at frequencies close to the maximum capability (fmax) of the transistor. However, the efficiency is low. Class-A PAs are therefore typically used in applications requiring low power, high linearity, high gain, broadband operation, or high-frequency operation.

The efficiency of real class-A PAs is degraded by the on-state resistance or saturation voltage of the transistor. It is also degraded by the presence of load reactance, which in essence requires the PA to generate more output voltage or current to deliver the same power to the load.

Class B

The gate bias in a class-B PA is set at the threshold of conduction so that (ideally) the quiescent drain current is zero. As a result, the transistor is active half of the time and the drain current is a half sinusoid. Since the amplitude of the drain current is proportional to drive amplitude and the shape of the drain-current waveform is fixed, class-B provides linear amplification.

The power output of a class-B PA is controlled by the drive level and varies as given by eq. (5). The DC-input current is, however, proportional to the drain current which is in turn proportional to the RF-output current. Consequently, the instantaneous efficiency of a class-B PA varies with the output voltage and for an ideal PA reaches $\pi/4$ (78.5 percent) at PEP. For low-level signals, class B is significantly more efficient than class A, and its average efficiency can be several times that of class A at high peak-to-average ratios (e.g., 28 vs. 5 percent for ξ = 10 dB). The utilization factor is the same 0.125 of class A.

In practice, the quiescent current is on the order of 10 percent of the peak drain current and adjusted to minimize crossover distortion caused by transistor nonlinearities at low outputs. Class B is generally used in a push-pull configuration so that the two drain-currents add together to produce a sine-wave output. At HF and VHF, the transformer-coupled push-pull topology (Figure 8) is generally used to allow broadband operation with minimum filtering. The use of the complementary topology (Figure 9) has generally been limited to audio, LF, and MF applications by the lack of suitable p-channel transistors. However, this topology is attractive for IC implementation and has recently been investigated for low-power applications at frequencies to 1 GHz [20].

Class C

In the classical (true) class-C PA, the gate is biased below threshold so that the transistor is active for less than half of the RF cycle (Figure 10). Linearity is lost, but efficiency is increased. The efficiency can be increased arbitrarily toward 100 percent by decreasing the conduction angle toward zero. Unfortunately, this causes the output power (utilization factor) to decrease toward zero and the drive power to increase toward infinity. A typical compromise is a conduction angle of 150° and an ideal efficiency of 85 percent.

The output filter of a true class-C PA is a parallel-tuned type that bypasses the harmonic components of the drain current to ground without generating harmonic voltages. When driven into saturation, efficiency is stabilized and the output voltage locked to supply voltage, allowing linear high-level amplitude modulation.

Classical class C is widely used in high-power vacuum-tube transmitters. It is, however, little used in solid-state PAs because it requires low drain resistances, making implementation of parallel-tuned output filters difficult. With BJTs, it is also difficult to set up bias and drive to produce a true class-C collector-current waveform. The use of a series-tuned output filter results in a mixed-mode class-C operation that is more like mistuned class E than true class C.

Class D

Class-D PAs use two or more transistors as switches to generate a square drain-voltage waveform. A series-tuned output filter passes only the fundamental-frequency component to the load, resulting in power outputs of $(8/\pi^2)V_{DD}^2/R$ and $(2/\pi^2)V_{DD}^2/R$ for the transformer-coupled and complementary configurations, respectively. Current is drawn only through the transistor that is on, resulting in a 100-percent efficiency for an ideal PA. The utilization factor ($1/2\pi = 0.159$) is the highest of any PA (27 percent higher than that of class A or B). A unique aspect of class D (with infinitely fast switching) is that efficiency is not degraded by the presence of reactance in the load.

Practical class-D PAs suffer from losses due to saturation, switching speed, and drain capacitance. Finite switching speed causes the transistors to be in their active regions while conducting current. Drain capacitances must be charged and discharged once per RF cycle. The associated power loss is proportional to $V_{DD}^3/2$ [21] and increases directly with frequency.

Class-D PAs with power outputs of 100 W to 1 kW are readily implemented at HF, but are seldom used above lower VHF because of losses associated with the drain capacitance. Recently, however, experimental class-D PAs have been tested with frequencies of operation as high as 1 GHz [22].

Class E

Class E employs a single transistor operated as a switch. The drain-voltage waveform is the result of the sum of the DC and RF currents charging the drain-shunt capacitance. In optimum class E, the drain voltage drops to zero and has zero slope just as the transistor turns on. The result is an ideal efficiency of 100 percent, elimination of the losses associated with charging the drain capacitance in class D, reduction of switching losses, and good tolerance of component variation.

Optimum class-E operation requires a drain shunt susceptance 0.1836/R and a drain series reactance 1.15R and delivers a power output of $0.577V_{DD}^2/R$ for an ideal PA [23]. The utilization factor is 0.098. Variations in load impedance and shunt susceptance cause the PA to deviate from optimum operation [24, 25], but the degradations in performance are generally no worse than those for class A and B.

The capability for efficient operation in the presence of significant drain capacitance makes class E useful in a number of applications. One example is high-efficiency HF PAs with power levels to 1 kW based upon low-cost MOSFETs intended for switching rather than RF use [26]. Another example is the switching-mode operation at frequencies as high as K band [27]. The class-DE PA [28] similarly uses dead-space between the times when its two transistors are on to allow the load network to charge/discharge the drain capacitances.

Class F

Class F boosts both efficiency and output by using harmonic resonators in the output network to shape the drain waveforms. The voltage waveform includes one or more odd harmonics and approximates a square wave, while the current includes even harmonics and approximates a half sine wave. Alternately (“inverse class F”), the voltage can approximate a half sine wave and the current a square wave. As the number of harmonics increases, the efficiency of an ideal PA increases from the 50 percent (class A) toward unity (class D) and the utilization factor increases from 1/8 (class A) toward $1/2\pi$ (class D) [29].

The required harmonics can in principle be produced by current-source operation of the transistor. However, in practice the transistor is driven into saturation during part of the RF cycle and the harmonics are produced by a self-regulating mechanism similar to that of saturating class C. Use of a harmonic voltage requires creating a high impedance (3 to 10 times the load impedance) at the drain, while use of a harmonic current requires a low impedance (1/3 to 1/10 of the load impedance). While class F requires a more complex output filter than other PAs, the impedances must be correct at only a few specific frequencies. Lumped-element traps are used at lower frequencies and transmission lines are used at microwave frequencies. Typically, a shorting stub is placed a quarter or half-wavelength away from the drain. Since the stubs for different harmonics interact and the open or short must be created at a “virtual drain” ahead of the drain capacitance and bond-wire inductance, implementation of suitable networks is a bit of an art. Nonetheless, class-F PAs are successfully implemented from MF through Ka band.

A variety of modes of operation in-between class C, E, and F are possi-

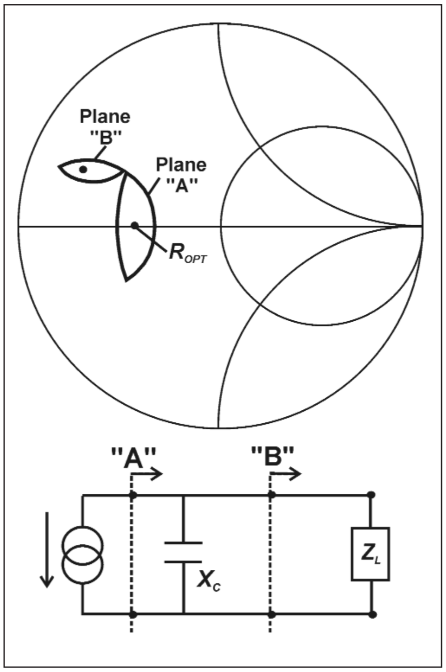

Figure 11 · Contant power contours and transformation.

ble. The maximum achievable efficiency [30] depends upon the number of harmonics, (0.5, 0.707, 0.8165, 0.8656, 0.9045 for 1 through 5 harmonics, respectively). The utilization factor depends upon the harmonic impedances and is highest for ideal class-F operation.

6b. LOAD-PULL CHARACTERIZATION

RF-power transistors are characterized by breakdown voltages and saturated drain currents. The combination of the resultant maximum drain voltage and maximum drain current dictates a range of load impedances into which useful power can be delivered, as well as an impedance for delivery of the maximum power. The load impedance for maximum power results in drain voltage and current excursions from near zero to nearly the maximum rated values.

The load impedances corresponding to delivery of a given amount of RF power with a specified maximum drain voltage lie along parallel-resistance lines on the Smith chart. The impedances for a specified maximum current analogously follow a series-resistance line. For an ideal PA, the resultant constant-power contour is football-shaped as shown in Figure 11.

In a real PA, the ideal drain is embedded behind the drain capacitance and bond-wire/package inductance. Transformation of the ideal drain impedance through these elements causes the constant-power contours to become rotated and distorted [31]. With the addition of second-order effects, the contours become elliptical. A set of power contours for a given PA somewhat resembles a set of contours for a conjugate match. However, a true conjugate match produces circular contours. With a power amplifier, the process is more correctly viewed as loading to produce a desired power output. As shown in the example of Figure 12, the power and efficiency contours are not necessarily aligned, nor do maximum power and maximum efficiency necessarily occur for the same load impedance. Sets of such “load-pull” contours are widely used to facilitate design trade-offs.

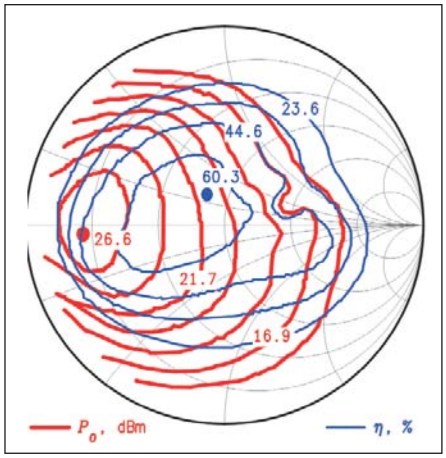

Figure 12 · Example load-pull contours for a 0.5-W, 836 MHz PA. (Courtesy Focus Microwaves and dBm Engineering)

Load-pull analyses are generally iterative in nature, as changing one parameter may produce a new set of contours. A variety of different parameters can be plotted during a load-pull analysis, including not only power and efficiency, but also distortion and stability. Harmonic impedances as well as drive impedances are also sometimes varied.

A load-pull system consists essentially of a test fixture, provided with biasing capabilities, and a pair of low-loss, accurately resettable tuners, usually of precision mechanical construction. A load-pull characterization procedure consists essentially of measuring the power of a device, to a given specification (e.g., the 1-dB compression point) as a function of impedance. Data are measured at a large number of impedances and plotted on a Smith chart. Such plots are, of course, critically dependent on the accurate calibration of the tuners, both in terms of impedance and losses. Such calibration is, in turn, highly dependent on the repeatability of the tuners.

Precision mechanical tuners, with micrometer-style adjusters, were the traditional apparatus for load-pull analysis. More recently, a new generation of electronic tuners has emerged that tune through the use varactors or transmission lines switched by pin diodes. Such electronic tuners [32] have the advantage of almost perfect repeatability and high tuning speed, but have much higher losses and require highly complex calibration routines. Mechanical tuners are more difficult to control using a computer, and move very slowly from one impedance setting to another.

In an active load-pull system, a second power source, synchronized in frequency and phase with the device input excitation, is coupled into the output of the device. By controlling the amplitude and phase of the injected signal, a wide range of impedances can be simulated at the output of the test device [33]. Such a system eliminates the expensive tuners, but creates a substantial calibration challenge of its own. The wide availability of turn-key load-pull systems has generally reduced the application of active load-pull to situations where mechanical or electronic tuning becomes impractical (e.g., millimeter-wave frequencies).

6c. STABILITY

The stability of a small-signal RF amplifier is ensured by deriving a set of S-parameters from using measured data or a linear model, and then establishing the value of the k-factor stability parameter. If the k-factor is greater than unity, at the frequency and bias level in question, then expressions for matching impedances at input and output can be evaluated to give a perfect conjugate match for the device. Amplifier design in this context is mainly a matter of designing matching networks which present the prescribed impedances over the necessary specified bandwidth. If the k factor is less than unity, negative feedback or lossy matching must be employed in order to maintain an unconditionally stable design.

A third case is relevant to PA design at higher microwave frequencies. There are cases where a device has a very high k-factor value, but very low gain in conjugate matched condition. The physical cause of this can be traced to a device which has gain roll-off due to carrier-mobility effects, rather than parasitics. In such cases, introduction of some positive feedback reduces the k-factor and increases the gain in conjugately matched conditions, while maintaining unconditional stability. This technique was much used in the early era of vacuum-tube electronics, especially in IF amplifiers.

6d. MICROWAVE IMPLEMENTATION

At microwave frequencies, lumped elements (capacitors, inductors) become unsuitable as tuning components and are used primarily as chokes and by-passes. Matching, tuning, and filtering at microwave frequencies are therefore accomplished with distributed (transmission-line) networks. Proper operation of power amplifiers at microwave frequencies is achieved by providing the required drain-load impedance at the fundamental and a number of harmonic frequencies.

Class F

Class-F operation is specified in terms of harmonic impedances, so it is relatively easy to see how transmission-line networks are used. Methods for using transmission lines in conjunction with lumped-element tuned circuits appear in the original paper by Tyler [34]. In modern microwave implementation, however, it is generally necessary to use transmission lines exclusively. In addition, the required impedances must be produced at a virtual ideal drain that is separated from the output network by drain capacitance, bond-wire/lead inductance.

Typically, a transmission line between the drain and the load provides the fundamental-frequency drain impedance of the desired value. A stub that is a quarter wavelength at the harmonic of interest and open at one end provides a short circuit at the opposite end. The stub is placed along the main transmission line at either a quarter or a half wavelength from the drain to create either an open or a short circuit at the drain [35]. The supply voltage is fed to the drain through a half-wavelength line bypassed on the power-supply end or alternately by a lumped-element choke. When multiple stubs are used, the stub for the highest controlled harmonic is placed nearest the drain. Stubs for lower harmonics are placed progressively further away and their lengths and impedances are adjusted to allow for interactions. Typically, “open” means three to ten times the fundamental-frequency impedance, and “shorted” means no more 1/10 to 1/3 of the fundamental-frequency impedance [FR17].

A wide variety of class-F PAs have been implemented at UHF and microwave frequencies [36-41]. Generally, only one or two harmonic impedances are controlled. In the X-band PA from [42], for example, the output circuit provides a match at the fundamental and a short circuit at the second harmonic. The third-harmonic impedance is high, but not explicitly adjusted to be open. The 3-dB bandwidth of such an output network is about 20 percent, and the efficiency remains within 10 percent of its maximum value over a bandwidth of approximately 10 to 15 percent.

Dielectric resonators can be used in lieu of lumped-element traps in class-F PAs. Power outputs of 40 W have been obtained at 11 GHz with efficiencies of 77 percent [43].

Class E

The drain-shunt capacitance and series inductive reactance required for optimum class-E operation result in a drain impedance of $R + j0.725R$ at the fundamental frequency, $-j1.7846R$ at the second harmonic, and proportionately smaller capacitive reactances at higher harmonics. At microwave frequencies, class-E operation is approximated by providing the drain with the fundamental-frequency impedance and preferably one or more of the harmonic impedances [44].

An example of a microwave approximation of class E that provides the correct fundamental and second-harmonic impedances [44] is shown in Figure 13. Line l2 is a quarter-wavelength long at the second harmonic so that the open circuit at its end is transformed to a short at plane AA'. Line l1 in combination with L and C is designed to be also a quarter wavelength to translate the short at AA' to an open at the transistor drain. The lines l1 to l4 provide the desired impedance at the funda-

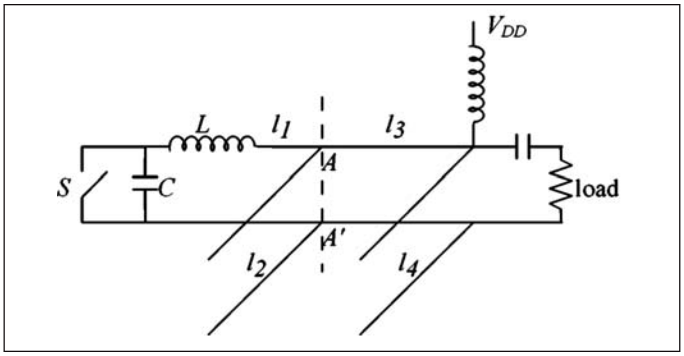

Figure 13 · Idealized microwave class-E PA circuit.

Figure 14 · Example X-band class-E PA.

mental. The implementation using an FLK052 MESFET is shown in Figure 14 produces 0.68 W at X band with a drain efficiency of 72 percent and PAE of 60 percent [42].

Methods exist for providing the proper impedances through the fourth harmonic [45]. However, the harmonic impedances are not critical [30], and many variations are therefore possible. Since the transistor often has little or no gain at the higher harmonic frequencies, those impedances often have little or no effect upon performance. A single-stub match is often sufficient to provide the desired impedance at the fundamental while simultaneously providing an adequately high impedance at the second harmonic, thus eliminating the need for an extra stub and reducing a portion of the losses associated with it. Most microwave class-E amplifiers operate in a suboptimum mode [46]. Demonstrated capabilities range from 16 W with 80-percent efficiency at UHF (LDMOS) to 100 mW with 60-percent efficiency at 10 GHz [47], [48], [44], [49], [50], [51]. Optical sampling of the waveforms [52] has verified that these PAs do indeed operate in class E.

Comparison

PAs configured for classes A (AB), E, and F are compared experimentally in [50] with the following conclusions. Classes AB and F have essentially the same saturated output power, but class F has about 15 percent higher efficiency. Class E has the highest efficiency. Gain compression occurs at a lower power level for class E than for class F. For a given efficiency, class F produces more power. For the same maximum output power, the third order intermodulation products are about 10 dB lower for class F than for class E. Lower-power PAs implemented with smaller RF power devices tend to be more efficient than PAs implemented with larger devices [42].

Millimeter-Wave PAs

Solid-state PAs for millimeter-wave (mm-W) frequencies (30 to 100 GHz) are predominantly monolithic. Most Ka-band PAs are based upon pHEMT devices, while most W-band PAs are based upon InP HEMTs. Some use is also made of HBTs at the lower mm-W frequencies. Class A is used for maximum gain. Typical performance characteristics include 4 W with 30-percent PAE at Ka band [53], 250 mW with 25-percent PAE at Q band [54], and 200 mW with 10-percent PAE at W band [55]. Devices for operation at mm-W are inherently small, so large power outputs are obtained by combining the outputs of multiple low-power amplifiers in corporate or spatial power combiners.

6e. EXAMPLE APPLICATIONS

The following examples illustrate the wide variety of power amplifiers in use today:

HF/VHF Single Sideband

One of the first applications of RF-power transistors was linear amplification of HF single-sideband signals. Many PAs developed by Helge Granberg have been widely adapted for this purpose [56, 57]. The 300-W PA for 2 to 30 MHz uses a pair of Motorola MRF422 Si NPN transistors in a push-pull configuration. The PA operates in class AB push-pull from a 28-V supply and achieves a collector efficiency of about 45 percent (CW) and a two-tone IMD ratio of about –30 dBc. The 1-kW amplifier is based upon a push-pull pair of MRF154 MOSFETs and operates from a 50-V supply. Over the frequency range of 2 to 50 MHz it achieves a drain efficiency of about 58 percent (CW) with an IMD rating of –30 dBc.

13.56-MHz ISM Power Sources

High-power signals at 13.56 MHz are needed for a wide variety of Industrial, Scientific, and Medical (ISM) applications such as plasma generation, RF heating, and semiconductor processing. A 400-W class-E PA uses an International Rectifier IRFP450LC MOSFET (normally used for low-frequency switching-mode DC power supplies) operates from a 120-V supply and achieves a drain efficiency of 86 percent [58, 26]. Industrial 13.56-MHz RF power generators using class-E output stages have been manufactured since 1992 by Dressler Hochfrequenztechnik (Stolberg, Germany) and Advanced

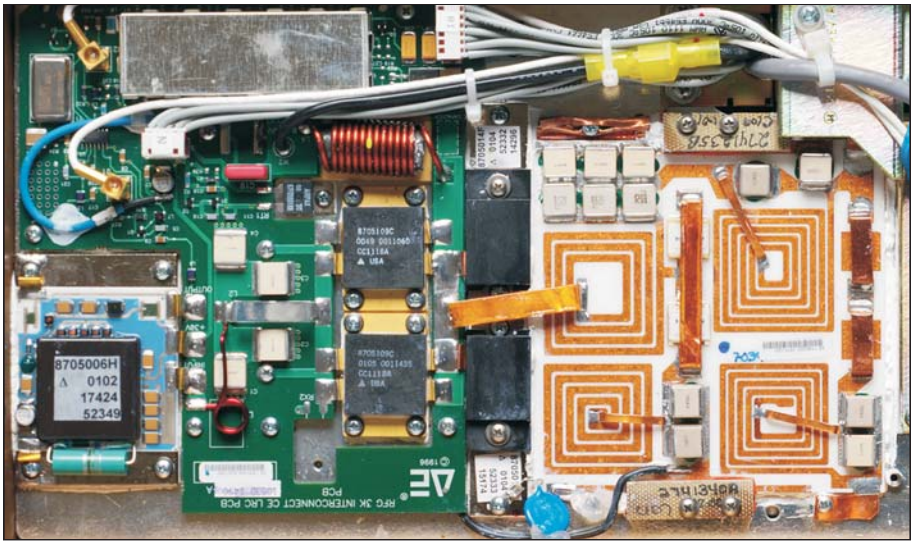

Figure 15 · 3-kW high efficiency PA for 13.56 ISM-band operation. (Courtesy Advanced Energy)

Figure 16 · Output section of a 50-kW AM broadcast transmitter. (Courtesy Harris)

Energy Industries (Ft. Collins, CO). They typically use RF-power MOSFETs with 500- to 900-V breakdown voltages made by Directed Energy or Advanced Power Technology and produce output powers of 500 W to with 3 kW with drain efficiencies of about 90 percent. The Advanced Energy Industries amplifier (Figure 15) uses thick-film-hybrid circuits to reduce size. This allows placement inside the clean-room facilities of semiconductor-manufacturing plants, eliminating the need for long runs of coaxial cable from an RF-power generator installed outside the clean-room.

VHF FM Broadcast Transmitter

FM-broadcast transmitters (88 to 108 MHz) with power outputs from 50 W to 10 kW are manufactured by Broadcast Electronics (Quincy, Illinois). These transmitters use up to 32 power-combined PAs based upon Motorola MRF151G MOSFETs. The PAs operate in class C from a 44-V supply and achieve a drain efficiency of 80 percent. Typically, about 6 percent of the output power is dissipated in the power combiners, harmonic-suppression filter, and lightning-protection circuit.

MF AM Broadcast Transmitters

Since the 1980s, AM broadcast transmitters (530 to 1710 kHz) have been made with class-D and -E RF-output stages. Amplitude modulation is produced by varying the supply voltage of the RF PA with a high-efficiency amplitude modulator.

Transmitters made by Harris (Mason, Ohio) produce peak-envelope output powers of 58, 86, 150, 300, and 550 kW (unmodulated carrier powers of 10, 15, 25, 50, and 100 kW). The 100-kW transmitter combines the output power from 1152 transistors. The output stages can use either bipolars or MOSFETs, typically operate in class DE from a 300-V supply, and achieve an efficiency of 98 percent. The output section of the Harris 3DX50 transmitter is shown in Figure 16.

Transmitters made by Broadcast Electronics (Quincy, IL) use class-E RF-output stages based upon APT6015LVR MOSFETs operating from 130-V maximum supply voltages. They achieve drain efficiencies of about 94 percent with peak-envelope output powers from 4.4 to 44 kW. The 44-kW AM-10A transmitter combines outputs from 40 individual output stages.

900-MHz Cellular-Telephone Handset

Most 900-MHz CDMA handsets use power-amplifier modules from vendors such as Conexant and RF Micro Devices. These modules typically contain a single GaAs-HBT RFIC that includes a single-ended class-AB PA. Recently developed PA modules also include a silicon control IC that provides the base-bias reference voltage and can be commanded to adjust the output-transistor base bias to optimize efficiency while maintaining acceptably low amplifier distortion. over the full ranges of temperature and output power. A typical module (Figure 17) produces 28 dBm (631 mW) at full output with a PAE of 35 to 50 percent.

Cellular-Telephone Base Station Transmitter

The Spectrian MCPA 3060 cellular base-station transmitter for 1840-1870 MHz CDMA systems provides up to 60-W output while transmitting a signal that may include as many 9 modulated carriers. IMD is minimized by linearizing a class-AB main amplifier with both adaptive predistortion and adaptive feed-forward cancellation. The adaptive control

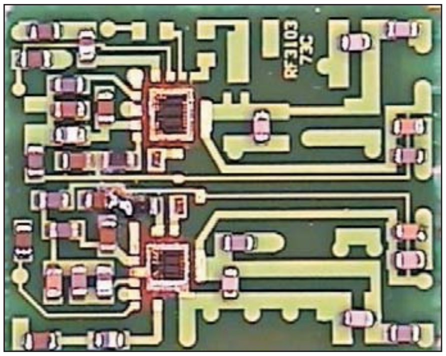

Figure 17 · Internal view of a dual-band (GSM/DCS) PA module for cellular telephone handsets. (Courtesy RF Micro Devices)

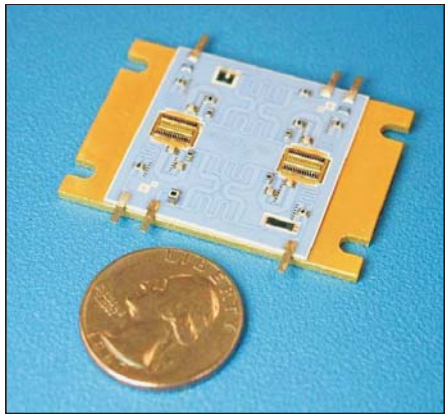

Figure 18 · Thick-film hybrid S-band PA module. (Courtesy UltraRF)

system adjusts operation as needed to compensate for changes due to temperature, time, and output power. The required adjustments are derived from continuous measurements of the system response to a spread-spectrum pilot test signal. The amplifier consumes a maximum of 810 W from a 27-V supply.

S-Band Hybrid Power Module

A thick-film-hybrid power-amplifier module made by UltraRF (now Cree Microwave) for 1805 to 1880 MHz DCS and 1930-1960 MHz PCS is shown in Figure 18. It uses four 140-mm LDMOS FETs operating from a 26-V drain supply. The individual PAs have 11-dB power gain and are quadrature-combined to produce a 100-W PEP output. The average output power is 40 W for EDGE and 7 W for CDMA, with an ACPR of –57 dBc for EDGE and –45 dBc for CDMA. The construction is based upon 0.02-in. thick film with silver metalization.

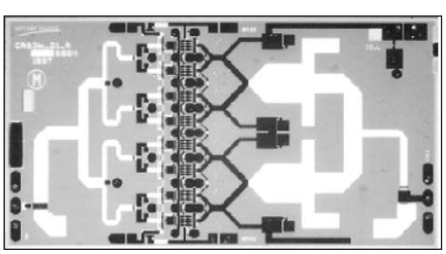

Figure 19 · MMIC PA for X- and K-bands.

GaAs MMIC Power Amplifier

A MMIC PA for use from 8 to 14 GHz is shown in Figure 19. This amplifier is fabricated with GaAs HBTs and intended for used in phased-array radar. It produces a 3-W output with a PAE of approximately 40 percent [59].

References

19. H. L. Krauss, C. W. Bostian, and F. H. Raab, *Solid State Radio Engineering,* New York: Wiley, 1980.

20. R. Gupta and D. J. Allstot, "Fully monolithic CMOS RF power amplifiers: Recent advances," *IEEE Communications Mag.*, vol. 37, no. 4, pp. 94-98, April 1999.

21. F. H. Raab and D. J. Rupp, "HF power amplifier operates in both class B and class D," *Proc. RF Expo West '93*, San Jose, CA, pp. 114-124, March 17-19, 1993.

22. P. Asbeck, J. Mink, T. Itoh, and G. Haddad, "Device and circuit approaches for next-generation wireless communications," *Microwave J.*, vol. 42, no. 2, pp. 22-42, Feb. 1999.

23. N. O. Sokal and A. D. Sokal, "Class E—a new class of high efficiency tuned single-ended switching power amplifiers," *IEEE J. Solid-State Circuits*, vol. SC-10, no. 3, pp. 168-176, June 1975.

24. F. H. Raab, "Effects of circuit variations on the class E tuned power amplifier," *IEEE J. Solid State Circuits*, vol. SC-13, no. 2, pp. 239-247, April 1978.

25. F. H. Raab, "Effects of VSWR upon the class-E RF-power amplifier," *Proc. RF Expo East '88*, Philadelphia, PA, pp. 299-309, Oct. 25-27, 1988.

26. J. F. Davis and D. B. Rutledge, "A low-cost class-E power amplifier with sine-wave drive," *Int. Microwave Symp. Digest*, vol. 2, pp. 1113-1116, Baltimore, MD, June 7-11, 1998.

27. T. B. Mader and Z. B. Popovic, "The transmission-line high-efficiency class-E amplifier," *IEEE Microwave and Guided Wave Letters*, vol. 5, no. 9, pp. 290-292, Sept. 1995.

28. D. C. Hamill, "Class DE inverters and rectifiers for DC-DC conversion," PESC96 Record, vol. 1, pp. 854-860, June 1996.

29. F. H. Raab, "Maximum efficiency and output of class-F power amplifiers," *IEEE Trans. Microwave Theory Tech.*, vol. 47, no. 6, pp. 1162-1166, June 2001.

30. F. H. Raab, "Class-E, -C, and -F power amplifiers based upon a finite number of harmonics," *IEEE Trans. Microwave Theory Tech.*, vol. 47, no. 8, pp. 1462-1468, Aug. 2001.

31. S. C. Cripps, *RF Power Amplifiers for Wireless Communication,* Norwood, MA: Artech, 1999.

32. "A load pull system with harmonic tuning," *Microwave J.*, pp. 128-132, March 1986.

33. B. Hughes, A. Ferrero, and A. Cognata, "Accurate on-wafer power and harmonic measurements of microwave amplifiers and devices," *IEEE Int. Microwave Symp. Digest*, Albuquerque, NM, pp. 1019-1022, June 1-5, 1992.

34. V. J. Tyler, "A new high-efficiency

Acronyms Used in Part 2

BJT	Bipolar Junction Transistor
DSP	Digital Signal Processor
IC	Integrated Circuit
IMD	Intermodulation Distortion
MOSFET	Metal Oxide Silicon FET

high power amplifier," *The Marconi Review*, vol. 21, no. 130, pp. 96-109, Fall 1958.

35. A. V. Grebennikov, "Circuit design technique for high-efficiency class-F amplifiers," *Int. Microwave Symp. Digest*, vol. 2, pp. 771-774, Boston, MA, June 13-15, 2000.

36. P. Colantonio, F. Giannini, G. Leuzzi, and E. Limiti, "On the class-F power-amplifier design," *RF and Microwave Computer-Aided Engin-eering*, vol. 32, no. 2, pp. 129-149, March 1999.

37. A. N. Rudiakova and V. G. Krizhanovski, "Driving waveforms for class-F power amplifiers," *Int. Microwave Symp. Digest*, vol. 1, pp. 473-476, Boston, MA, June 13-15, 2000.

38. A. Inoue, T. Heima, A. Ohta, R. Hattori, and Y. Mitsui, "Analysis of class-F and inverse class-F amplifiers," *Int. Microwave Symp. Digest*, vol. 2, pp. 775-778, Boston, MA, June 13-15, 2000.

39. F. van Rijs et al., "Influence of output impedance on power added efficiency of Si-bipolar power transistors," *Int. Microwave Symp. Digest*, vol. 3, pp. 1945-1948, Boston, MA, June 13-15, 2000.

40. F. Huin, C. Duvanaud, V. Serru, F. Robin, and E. Leclerc, "A single supply very high power and efficiency integrated PHEMT amplifier for GSM applications," *Proc. 2000 RFIC Symp.*, Boston, MA, CD-ROM, June 11-13, 2000.

41. B. Ingruber et al., "Rectangularly driven class-A harmonic-control amplifier," *IEEE Trans. Microwave Theory Tech.*, pt. 1, vol. 46, no. 11, pp. 1667-1672, Nov. 1998.

42. E. W. Bryerton, M. D. Weiss, and Z. Popovic, "Efficiency of chip-level versus external power combining," *IEEE Trans. Microwave Theory Tech.*, vol. 47, no. 8, pp. 1482-1485, Aug. 1999.

43 S. Toyoda, "Push-pull power amplifiers in the X band," *Int. Microwave Symp. Digest*, vol. 3, pp. 1433-1436, Denver, CO, June 8-13, 1997.

44. T. B. Mader and Z. Popovic, "The transmission-line high-efficiency class-E amplifier," *IEEE Micro-wave and Guided Wave Lett.*, vol. 5, no. 9, pp. 290-292, Sept. 1995.

45. A. J. Wilkinson and J. K. A. Everard, "Transmission line load network topology for class E amplifiers," *IEEE Trans. Microwave Theory Tech.*, vol. 47, no. 6, pp. 1202-1210, June 2001.

46. F. H. Raab, "Suboptimum operation of class-E power amplifiers," *Proc. RF Technology Expo.*, Santa Clara, CA, pp. 85-98, Feb. 1989.

47. S. Li, "UHF and X-band class-E amplifiers," Ph.D. Thesis, California Institute of Technology, Pasadena, 1999.

48. F. J. Ortega-Gonzalez, J. L. Jimenez-Martin, A. Asensio-Lopez, G. Torregrosa-Penalva, "High-efficiency load-pull harmonic controled class-E power amplifier," *IEEE Microwave Guided Wave Lett.*, vol. 8, no. 10, pp. 348-350, Oct. 1998.

49. E. Bryerton, "High-efficiency switched-mode microwave circuits," Ph.D. dissertation, Univ. of Colorado, Boulder, June 1999.

50. T. B. Mader, E. W. Bryerton, M. Markovic, M. Forman, and Z. Popovic, "Switched-mode high-efficiency microwave power amplifiers in a free-space power-combiner array," *IEEE Trans. Microwave Theory Tech.*, vol. 46, no. 10, pt. I, pp. 1391-1398, Oct. 1998.

51. M. D. Weiss and Z. Popovic, "A 10 GHz high-efficiency active antenna," *Int. Microwave Symp. Digest*, vol. 2, pp. 663-666, Anaheim, CA, June 14-17, 1999.

52. M. Weiss, M. Crites, E. Bryerton, J. Whitacker, and Z. Popovic, ""Time domain optical sampling of nonlinear microwave amplifiers and multipliers," *IEEE Trans. Microwave Theory Tech.*, vol. 47, no.12, pp. 2599-2604, Dec. 1999.

53. J. J. Komiak, W. Kong, P. C. Chao, and K. Nichols, "Fully monolithic 4 watt high efficiency Ka-band power amplifier," *Int. Microwave Symp. Digest*, vol. 3, pp. 947-950, Anaheim, CA, June 14-17, 1999.

54. S.-W. Chen et al., "A 60-GHz high-efficiency monolithic power amplifier using 0.1-µm pHEMTs," *IEEE Microwave and Guided Wave Lett.*, vol.5, pp. 201-203, June 1995.

55. D. L. Ingram et al., "Compact W-band solid-state MMIC high power sources," *Int. Microwave Symp. Digest*, vol. 2, pp. 955-958, Boston, MA, June 13-15, 2000.

56. H. Granberg, "Get 300 watts PEP linear across 2 to 30 MHz from this push-pull amplifier," Bulletin EB27A, Motorola Semiconductor Products, Phoenix, Feb. 1980.

57. H. Granberg, "A compact 1-kW 2-50 MHz solid-state linear amplifier," *QEX*, no. 101, pp. 3-8, July 1990. Also AR347, Motorola Semiconductor Products, Feb. Oct. 1990.

58. N. O. Sokal, "Class-E RF power amplifiers ... ," *QEX*, No. 204, pp. 9-20, Jan./Feb. 2001.

59. M. Salib, A. Gupta, A. Ezis, M. Lee, and M. Murphy, "A robust 3W high efficiency 8-14 GHz GaAs/AlGaAs heterojunction bipolar transistor power amplifier," *Int. Microwave Symp. Digest*, vol. 2, pp. 581-584, Baltimore, MD, June 7-11, 1998.

Author Information

The authors of this series of articles are: Frederick H. Raab (lead author), Green Mountain Radio Research, e-mail: f.raab@ieee.org; Peter Asbeck, University of California at San Diego; Steve Cripps, Hywave Associates; Peter B. Kenington, Andrew Corporation; Zoya B. Popovic, University of Colorado; Nick Pothecary, Consultant; John F. Sevic, California Eastern Laboratories; and Nathan O. Sokal, Design Automation. Readers desiring more information should contact the lead author.

Notes

1. In Part 1 of this series (May 2003 issue), the references contained in Table 1 were not numbered correctly. The archived version has been corrected and may be downloaded from: www.highfrequencyelectronics.com — click on "Archives," select "May 2003 — Vol. 2 No. 3" then click on the article title.

2. This series has been extended to five parts, to be published in successive issues through January 2004.

RF and Microwave Power Amplifier and Transmitter Technologies — *Part 3*

By Frederick H. Raab, Peter Asbeck, Steve Cripps, Peter B. Kenington, Zoya B. Popovich, Nick Pothecary, John F. Sevic and Nathan O. Sokal

Transmitter architectures is the subject of this installment of our continuing series on power amplifiers, with an emphasis on designs that can meet today's linearity and high efficiency requirements

The building blocks used in transmitters are not only power amplifiers, but a variety of other circuit elements including oscillators, mixers, low-level amplifiers, filters, matching networks, combiners, and circulators. The arrangement of building blocks is known as the architecture of a transmitter. The classic transmitter architecture is based upon linear PAs and power combiners. More recently, transmitters are being based upon a variety of different architectures including stage bypassing, Kahn, envelope tracking, outphasing, and Doherty. Many of these are actually fairly old techniques that have been recently made practical by the capabilities of DSP.

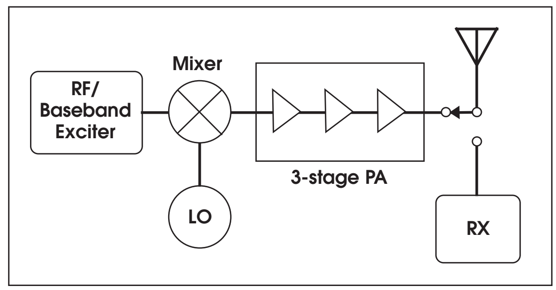

Figure 20 · A conventional transmitter.

7a. LINEAR ARCHITECTURE

The conventional architecture for a linear microwave transmitter consists of a baseband or IF modulator, an up-converter, and a power-amplifier chain (Figure 20). The amplifier chain consists of cascaded gain stages with power gains in the range of 6 to 20 dB. If the transmitter must produce an amplitude-modulated or multi-carrier signal, each stage must have adequate linearity. This generally requires class-A amplifiers with substantial power back-off for all of the driver stages. The final amplifier (output stage) is always the most costly in terms of device size and current consumption, hence it is desirable to operate the output stage in class B. In applications requiring very high linearity, it is necessary to use class A in spite of the lower efficiency.

The outputs of a driver stage must be matched to the input of the following stage much as the final amplifier is matched to the load. The matching tolerance for maintaining power level can be significantly lower than that for gain [60], hence the 1-dB load-pull contours are more tightly packed for power than for gain.

To obtain even modest bandwidths (e.g., above 5 percent), the use of quadrature balanced stages is advisable (Figure 21). The main benefit of the quadrature balanced configuration is that reflections from the transistors are cancelled by the action of the input and output couplers. An individual device can therefore be deliberately mismatched (e.g., to achieve a power match on the output), yet the quadrature-combined system appears to be well-matched. This configuration also acts as an effective power combiner, so that a given power rating can be achieved using a pair of devices having half of the required power performance. For moderate-bandwidth designs, the lower-power stages are typically designed using a simple single-ended cascade, which in some cases is available as an RFIC. Designs with bandwidths approaching an octave or

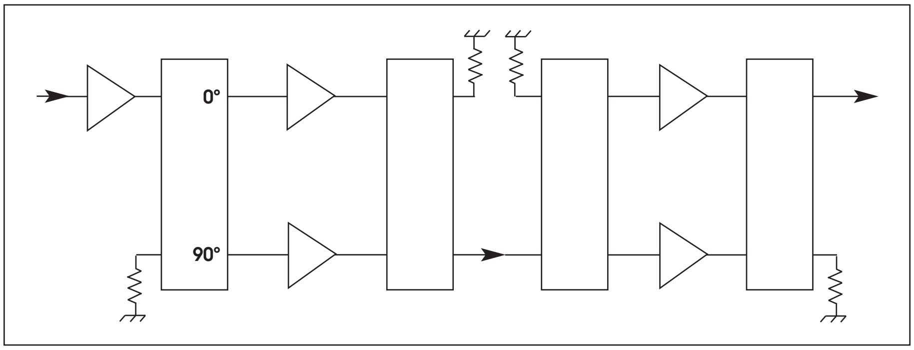

Figure 21 · Amplifier stages with quadrature combiners.

more require the use of quadrature-balanced stages throughout the entire chain.

Simple linear-amplifier chains of this kind have high linearity but only modest efficiency. Single-carrier applications usually operate the final amplifier to about the 1-dB compression point on amplitude modulation peaks. A thus-designed chain in which only the output stage exhibits compression can still deliver an ACPR in the range of about –25 dBc with 50-percent efficiency at PEP.

Two practical problems are frequently encountered in the design of linear PA chains: stability and low gain. Linear, class-A chains are actually more susceptible to oscillation due to their high gain, and single-path chains are especially prone to unstable behavior. Instability can be subdivided into the two distinct categories: Low-frequency oscillation and in-band instability. In-band instability is avoided by designing the individual gain stages to meet the criteria for unconditional stability; i.e., the Rollet *k* factor [61] must be greater than unity for both in-band and out-of-band frequencies. Meeting this criterion usually requires sacrificing some gain through the use of absorptive elements. Alternatively, the use of quadrature balanced stages provides much greater isolation between individual stages, and the broadband response of the quadrature couplers can eliminate the need to design the transistor stage itself with $k>1$. This is another reason for using quadrature coupled stages in the output of the chain.

Large RF power devices typically have very high transconductance, and this can produce low-frequency instability unless great care is taken to terminate both the input and output at low frequencies with impedances for unconditional stability. Because of large separation from the RF band, this is usually a simple matter requiring a few resistors and capacitors.

At X band and higher, the power gain of devices in the 10 W and above category can drop well below 10 dB. To maintain linearity, it may be necessary to use a similarly size device as a driver. Such an architecture clearly has a major negative impact upon the cost and efficiency of the whole chain. In the more extreme cases, it may be advantageous to consider a multi-way power combiner, where 4, 8, or an even greater number of smaller devices are combined. Such an approach also has other advantages, such as soft failure, better thermal management, and phase linearity. However, it typically consumes more board space.

7b. POWER COMBINERS

The need frequently arises to combine the outputs of several individual PAs to achieve the desired transmitter output. Whether to use a number of smaller PAs vs. a single larger PA is one of the most basic decisions in selection of an architecture [60]. Even when larger devices are available, smaller devices often offer higher gain, a lower matching *Q* factor (wider bandwidth), better phase linearity, and lower cost. Heat dissipation is more readily accomplished with a number of small devices, and a soft-failure mode becomes possible. On the other hand, the increase in parts count, assembly time, and physical size are significant disadvantages to the use of multiple, smaller devices.

Direct connection of multiple PAs is generally impractical as the PAs interact, allowing changes in output from one to cause the load impedance seen by the other to vary. A constant load impedance, hence isolation of one PA from the other, is provided by a hybrid combiner. A hybrid combiner causes the difference between the two PA outputs to be routed to and dissipated in a balancing or "dump" resistor. In the event that one PA fails, the other continues to operate normally, with the transmitter output reduced to one fourth of nominal.

The most common power combiner is the quadrature-hybrid combiner. A 90° phase shift is introduced at input of one PA and also at the output of the other. The benefits of quadrature combining include constant input impedance in spite of variations of input impedances of the individual PAs, cancellation of odd harmonics, and cancellation of backward-IMD (IMD resulting from a signal entering the output port). In addition, the effect of load impedance upon the system output is greatly reduced (e.g., to 1.2 dB for a 3:1 SWR). Maintenance of a nearly constant output occurs because the load impedance presented to one PA decreases when that presented to the other PA increases. As a result, however, device ratings increase and efficiency decreases roughly in proportion to the SWR [65]. Because quadrature combiners are inherently two-terminal devices, they are used in a corporate combining architecture

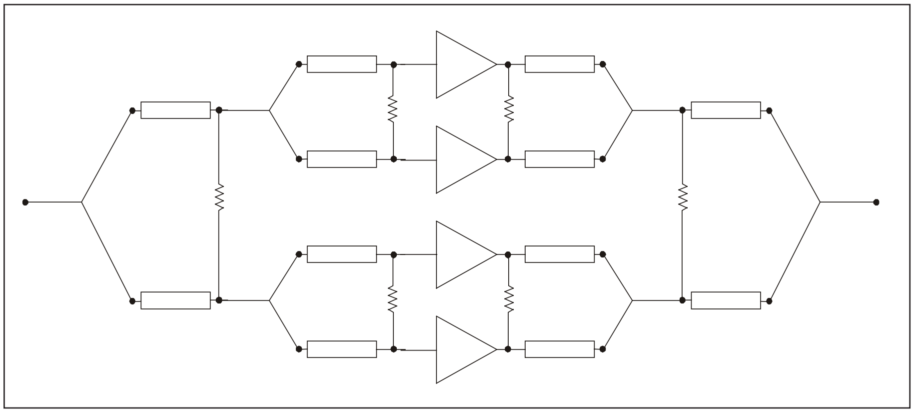

Figure 22 · Multi-section Wilkinson combining architecture.

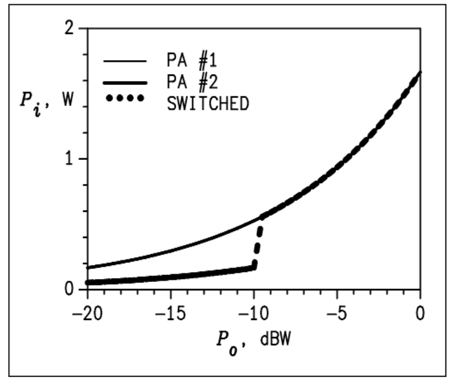

Figure 23 · Power consumption by PAs of different sizes.

(Figure 21). Unfortunately, the physical construction of such couplers poses some problems in a PC-board environment. The very tight coupling between the two quarter-wave transmission lines requires either very fine gaps or a three-dimensional structure. This problem is circumvented by the use of a miniature co-axial cable having a pair of precisely twisted wires to from the coupling section or ready-made, low-cost surface mount 3-dB couplers.

The Wilkinson or in-phase power combiner [62] is often more easily fabricated than a quadrature combiner. In the two-input form (as in each section in Figure 22), the outputs from two quarter-wavelength lines summed into load R_0 produce an apparent load impedance of $2R_0$, which is transformed through the lines into at the load impedances R_{PA} seen by the individual PAs. The difference between the two PA outputs is dissipated in a resistor connected across the two inputs. Proper choice of the balancing resistor ($2R_{PA}$) produces a hybrid combiner with good isolation between the two PAs. The Wilkinson concept can be extended to include more than two inputs [63].

Greater bandwidth can be obtained by increasing the number of transforming sections in each signal path. A single-section combiner can have a useful bandwidth of about 20 percent, whereas a two-section version can have a bandwidth close to an octave. In practice, escalating circuit losses generally preclude the use of more than two sections.

All power-combining techniques all suffer from circuit losses as well as mismatch losses. The losses in a simple two-way combiner are typically about 0.5 dB or 10 percent. For a four-way corporate structure, the interconnects typically result in higher losses. Simple open microstrip lines are too lossy for use in combining structures. One technique that offers a good compromise among cost, produceability, and performance, uses suspended stripline. The conductors are etched onto double-sided PC board, interconnected by vias, and then suspended in a machined cavity. Structures of this kind allow high-power 8-way combiners with octave bandwidths and of 0.5 dB.

A wide variety of other approaches to power-combining circuits are possible [62, 64]. Microwave power can also be combined during radiation from multiple antennas through "quasi-optical" techniques [66].

7c. STAGE SWITCHING AND BYPASSING

The power amplifier in a portable transmitter generally operates well below PEP output, as discussed in Section 4 (Part 1). The size of the transistor, quiescent current, and supply voltage are, however, determined by the peak output of the PA. Consequently, a PA with a lower peak output produces low-amplitude signals more efficiently than does a PA with a larger peak output, as illustrated in Figure 23 for class-B PAs with PEP efficiencies of 60 percent. Stage-bypassing and gate-switching techniques [67, 68] reduce power consumption and increase efficiency by switching between large and small amplifiers according to signal level. This process is analogous to selection of supply voltage in a class-G PA, and the average efficiency can be similarly computed [69].

A typical stage-bypassing architecture is shown in Figure 24. For low-power operation, switches SA and SB route the drive signal around the final amplifier.

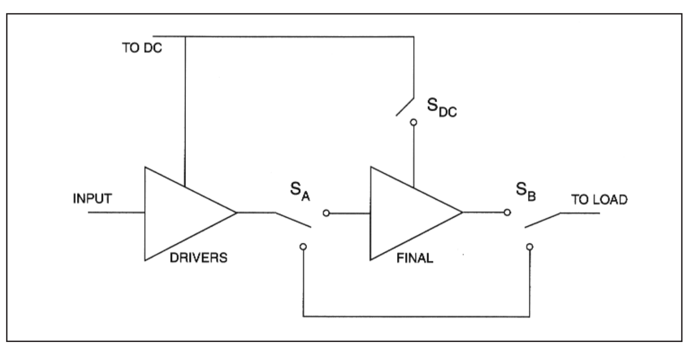

Figure 24 · Stage-bypassing architecture.

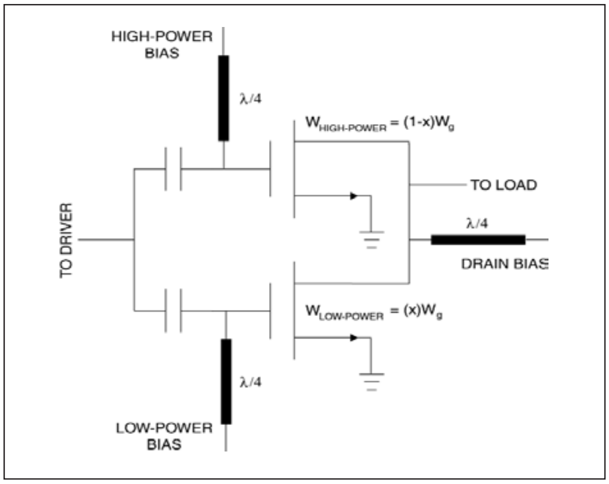

Figure 25 · Adaptive gate switching.

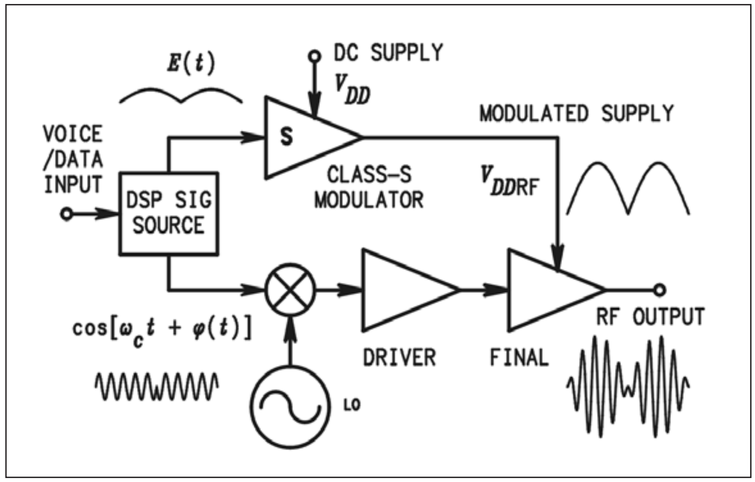

Figure 26 · Kahn-technique transmitter.

Simultaneously, switch SDC turns-off DC power to the final amplifier. The reduction in power consumption can improve the average efficiency significantly (e.g., from 2.1 to 9.5 percent in [70]). The control signal is based upon the signal envelope and power level (back-off). Avoiding hysteresis effects and distortion due to switching transients are critical issues in implementation.

A PA with adaptive gate switching is shown in Figure 25. The gate width (hence current and power capability) of the upper FET is typically ten to twenty times that of the lower FET. The gate bias for the high-power FET keeps it turned off unless it is needed to support a high-power output. Consequently, the quiescent drain current is reduced to low levels unless actually needed. The advantages of this technique are the absence of loss in the switches required by stage bypassing, and operation of the low-power FET in a more linear region (vs. varying the gate bias of a single large FET). The disadvantage is that the source and load impedances change as the upper FET is switched on and off.

7d. KAHN TECHNIQUE

The Kahn Envelope Elimination and Restoration (EER) technique (Figure 26) combines a highly efficient but nonlinear RF power amplifier (PA) with a highly efficient envelope amplifier to implement a high-efficiency linear RF power amplifier. In its classic form [73], a limiter eliminates the envelope, allowing the constant-amplitude phase modulated carrier to be amplified efficiently by class-C, -D, -E, or -F RF PAs. Amplitude modulation of the final RF PA restores the envelope to the phase-modulated carrier creating an amplified replica of the input signal.

EER is based upon the equivalence of any narrowband signal to simultaneous amplitude (envelope) and phase modulations. In a modern implementation, both the envelope and the phase-modulated carrier are generated by a DSP. In contrast to linear amplifiers, a Kahn-technique transmitter operates with high efficiency over a wide dynamic range and therefore produces a high average efficiency for a wide range of signals and power (back-off) levels. Average efficiencies three to five times those of linear amplifiers have been demonstrated (Figure 27) from HF [74] to L band [75].

Transmitters based upon the Kahn technique generally have excellent linearity because linearity depends upon the modulator rather than RF power transistors. The two most important factors affecting the linearity are the envelope bandwidth and alignment of the envelope and phase modulations. As a rule of thumb, the envelope bandwidth must be at least twice the RF bandwidth and the misalignment must not exceed one tenth of the inverse of the RF bandwidth [76]. In practice, the drive is not hard-limited as in the classical implementation. Drive power is conserved by allowing the drive to follow the envelope except at low levels. The use of a minimum drive level ensures proper operation of the RF PA at low signal levels where the gain is low [77]. At higher microwave frequencies, the RF power devices exhibit softer saturation characteristics and larger amounts of amplitude-to-phase conversion, necessitating the use of predistortion for good linearity [78].

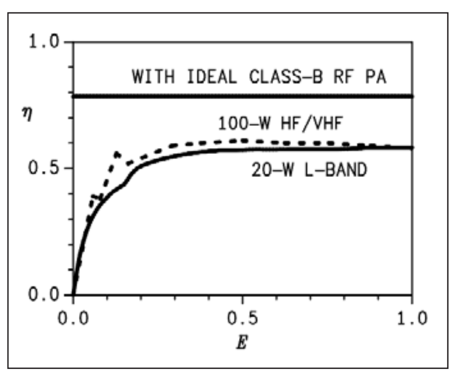

Figure 27 · Efficiency of Kahn-tecnique transmitters.

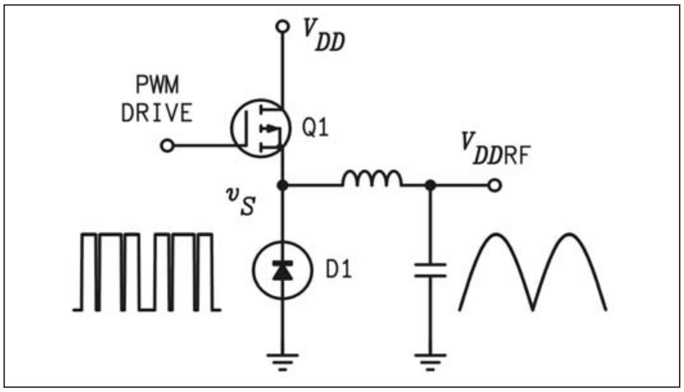

Figure 28 · Class-S modulator.

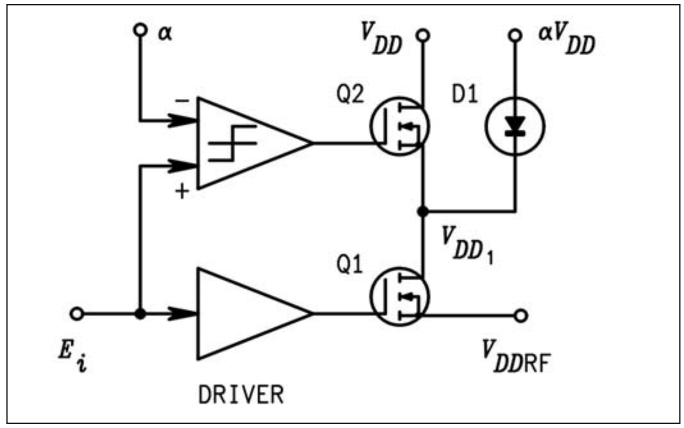

Figure 29 · Class-G modulator.

Class-S Modulator

A class-S modulator (Figure 28) uses a transistor and diode or a pair of transistors act as a two-pole switch to generate a rectangular waveform with a switching frequency several times that of the output signal. The width of pulses is varied in proportion to the instantaneous amplitude of the desired output signal, which is recovered by a low-pass filter. Class S is ideally 100 percent efficient and in practice can have high efficiency over a wide dynamic range. Class-S modulators are typically used as parts of a Kahn-technique transmitter, while class-S amplifiers are becoming popular for the efficient production of audio power in portable equipment. A class-S modulator can be driven by a digital (on/off) signal supplied directly from a DSP, eliminating the need for intermediate conversion to an analog signal.

Selection of the output filter is a compromise between passing the infinite-bandwidth envelope and rejecting FM-like spurious components that are inherent in the PWM process. Typically, the switching frequency must be six to seven times the RF bandwidth. Modulators with switching frequencies of 500 kHz are readily implemented using discrete MOSFETs and off-the-shelf ICs [74], while several MHz can be achieved using MOS ASICs or discrete GaAs devices [75].

Class-G Modulator

A class-G modulator (Figure 29) is a combination of linear series-pass (class-B) amplifiers that operate from different supply voltages. Power is conserved by selecting the one with the lowest useable supply voltage [69] so that the voltage drop across the active device is minimized.

Split-Band Modulator

Most of the power in the envelope resides at lower frequencies; typically 80 percent is in the DC component. The bandwidth of a class-S modulator can therefore be extended by combining it with a linear amplifier. While there are a number of approaches, the highest efficiency (typically 90 percent) is achieved by a diplexing combiner. Obtaining a flat frequency response and resistive loads for the two PAs is achieved by splitting the input signals in a DSP that acts as a pair of negative-component filters (Figure 30) [79]. The split-band modulator should make possible Kahn-technique transmitters with RF bandwidths of tens or even hundreds of MHz.

7e. ENVELOPE TRACKING

The envelope-tracking architecture (Figure 31) is similar to that of the Kahn technique. However, the final amplifier operates in a linear mode and the supply voltage is varied dynamically to conserve power [81, 82]. The RF drive contains both amplitude and phase information, and the burden of providing linear amplification lies entirely on the final RF PA. The role of the variable power supply is only to optimize efficiency.

Typically, the envelope is detected and used to control a DC-DC converter. While both buck (step-down) or boost (step-up) converters are used, the latter is more common as it allows operation of the RF PA from a supply voltage higher than the DC-supply voltage. This configuration is

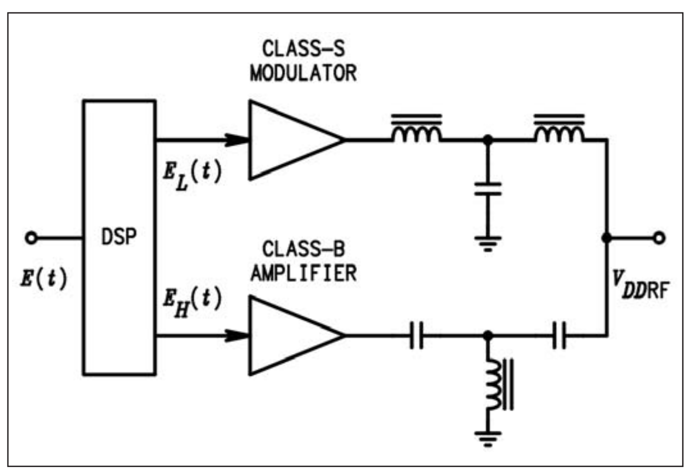

Figure 30 · Split-band modulator.

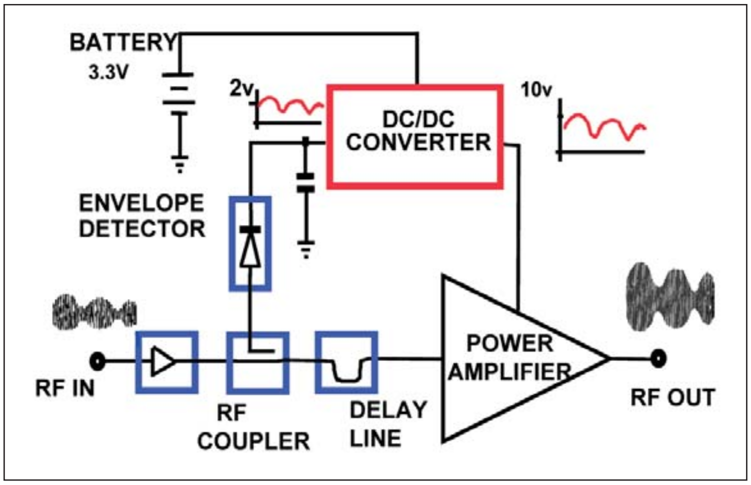

Figure 31 · Envelope-tracking architecture.

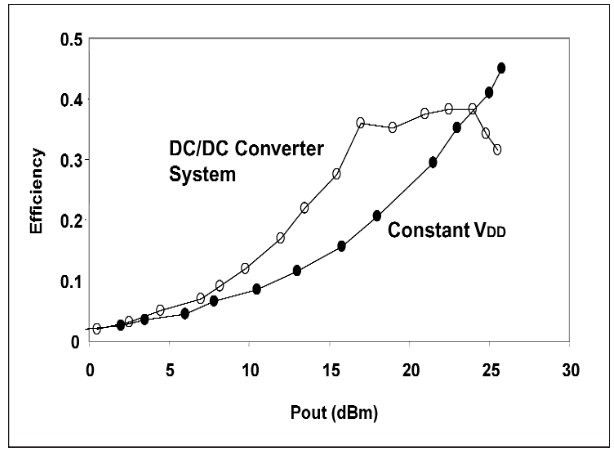

Figure 32 · Efficiency of a GaAs FET envelope-tracking transmitter.

also more amenable to the use of *npn* or *n*-channel transistors for fast switching. The result is a minimum V_{DDRF} corresponding to the DC-supply voltage and tracking of larger envelopes with a fixed "headroom" to ensure linear operation of the RF PA. If the RF PA is operated in class A, its quiescent current can also be varied.

In general, excess power-supply voltage translates to reduced efficiency, rather than output distortion. In principle, perfect tracking of the envelope by the supply voltage preserves the peak efficiency of the RF PA for all output amplitudes, as in the Kahn technique. In practice, efficiency improvement is obtained over a limited range of output power.

A high switching frequency in the DC-DC converter allows both a high modulation bandwidth and the use of smaller inductors and capacitors. The switching devices in the converter can in fact be implemented using the same same transistor technology used in the RF PA. Converters with switching frequencies of 10 to 20 MHz have recently been implemented using MOS ASICs [80], GaAs HBTs [83, 84] and RF power MOSFETs [85].

Representative results for an envelope-tracking transmitter based on a GaAs FET power amplifier are shown in Figure 32. The efficiency is lower at high power than that of the conventional amplifier with constant supply voltage due to the inefficiency of the DC-DC converter. However, the efficiency is much higher over a wide range of output power, with the average efficiency approximately 40 percent higher than that of the conventional linear amplifier.

Spurious outputs can be produced by supply-voltage ripple at the switching frequency. The effects of the ripple can be minimized by making the switching frequency sufficiently high or by using an appropriate filter. Variation of the RF PA gain with supply voltage can introduce distortion. Such distortion can, however, be countered by predistortion techniques [to be covered in Section 8 (Part 4)].

7f. OUTPHASING

Outphasing was invented during the 1930s as a means of obtaining high-quality AM from vacuum tubes with poor linearity [86] and was used through about 1970 in RCA "Ampliphase" AM-broadcast transmitters. In the 1970s, it came into use at microwave frequencies under the name "LINC" (Linear Amplification using Nonlinear Components) [87].

An outphasing transmitter (Figure 33) produces an amplitude-modulated signal by combining the outputs of two PAs driven with signals of different time-varying phases. Basically, the phase modulation causes the instantaneous vector sum of the two PA outputs to follow the desired signal amplitude (Figure 34). The inverse sine of envelope E phase-modulates the driving signals for the two PAs to produce a transmitter output that is proportional to E. In a modern implementation, a DSP and synthesizer produce the inverse-sine modulations of the driving signals.

Hybrid combining (Figure 33) isolates the PAs from the reactive loads inherent in outphasing, allowing them to see resistive loads at all signal levels. However, both PAs deliver full power all of the time. Consequently, the efficiency of a hybrid-coupled outphasing transmitter varies with the output power (Figure 35), resulting in an average efficiency that is inversely proportional to peak-to-average ratio (as for class A). Recovery of the power from the dump port of the hybrid combiner offers some improvement in the efficiency [88].

The phase of the output current is that of the vector sum of the two PA-output voltages. Direct summation of the out-of-phase signals in a nonhybrid combiner inherently results in reactive load impedances for the power amplifiers [89]. If the reactances are not partially cancelled as in the Chireix technique, the current drawn from the PAs is proportional to the transmitter-output voltage.

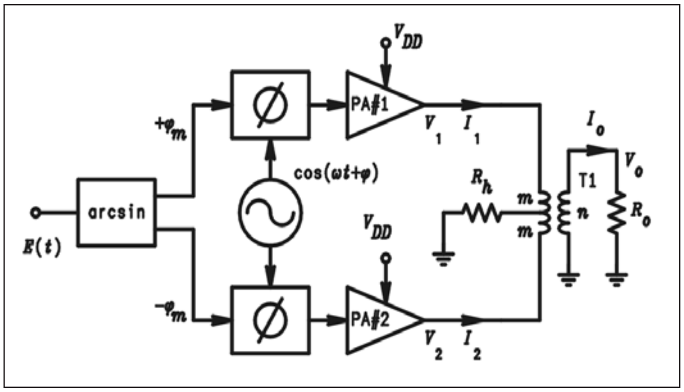

Figure 33 · Hybrid-combined outphasing transmitter.

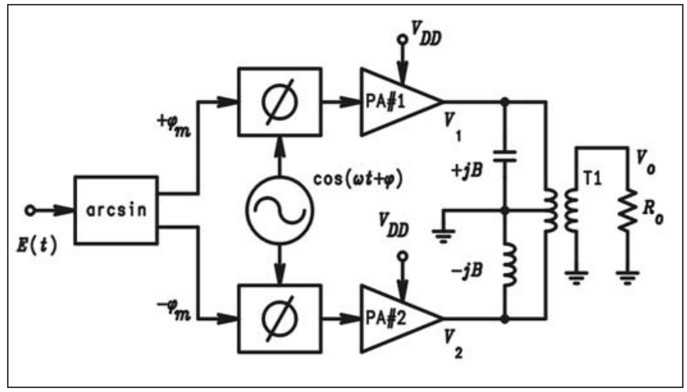

Figure 36 · Chireix-outphasing transmitter.

This results in an efficiency characteristic similar to that of a class-B PA.

The Chireix technique [86] uses shunt reactances on the inputs to the combiner (Figure 36) to tune-out the drain reactances at a particular amplitude, which in turn maximizes the efficiency in the vicinity of that amplitude. The efficiency at high and low amplitudes may be degraded. In the classic Chireix implementation, the shunt reactances maximize the efficiency at the level of the unmodulated carrier in an AM signal and produce good efficiency over the upper 6 dB of the output range. With judicious choice of the shunt susceptances, the average efficiency can be maximized for any given signal [89, 90]. For example, a normalized susceptance of 0.11 peaks the instantaneous efficiency at a somewhat lower amplitude, resulting in an average efficiency of 52.1 percent for an ideal class-B PA and a 10-dB Rayleigh-envelope signal (vs. 28 percent for linear amplification).

Virtually all microwave outphasing systems in use today are of the hybrid-coupled type. Use of the Chireix technique at microwave frequencies is difficult because microwave PAs do not behave as ideal voltage sources. Simulations suggest that direct (nonhybrid) combining increases both efficiency and distortion [91]. Since outphasing offers a wide bandwidth and the distortion can be mitigated by techniques such as predistortion, directly coupled and Chireix techniques should be fruitful areas for future investigation.

7g. DOHERTY TECHNIQUE

Development of the Doherty technique in 1936 [92] was motivated by the observation that signals with significant amplitude modulation resulted in low average efficiency. The classical Doherty architecture (Figure 37) combines two PAs of equal capacity through quarter-wave-length lines or networks. The "carrier" (main) PA is biased in class B while the "peaking" (auxiliary) PA is biased in class C. Only the carrier PA is active when the signal amplitude is half or less of the PEP amplitude. Both PAs contribute output power when the signal amplitude is larger than half of the PEP amplitude

Operation of the Doherty system can be understood by dividing it into low-power, medium-power (load-modulation), and peak-power regions [96]. The current and voltage relationships are shown in Figure 38 for ideal transistors and lossless matching networks. In the low-power region, the instantaneous amplitude of the input signal is insufficient to overcome the class-C (negative) bias of the peaking PA, thus the peaking PA remains cut-off and appears as an open-circuit. With the example load impedances shown in Figure 37, the carrier PA sees a 100 ohm load and operates as an ordinary class-B amplifier. The drain voltage increases linearly with output until reaching supply voltage V_{DD}. The instantaneous efficiency at this point (–6 dB from PEP) is therefore the 78.5 percent of the ideal class-B PA.

As the signal amplitude increases into the medium-power region, the carrier PA saturates and the peaking PA becomes active. The additional current I_2 sent to the load by the peaking PA causes the apparent load impedance at V_L to increase above

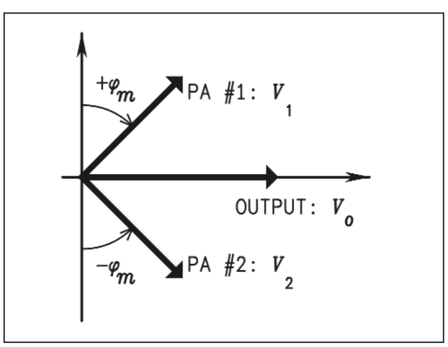

Figure 34 · Signal vectors in outphasing.

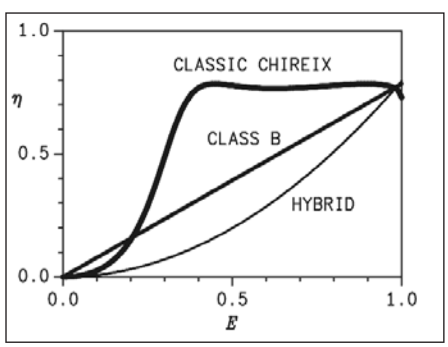

Figure 35 · Efficiency of outphasing transmitters with ideal class-B PAs.

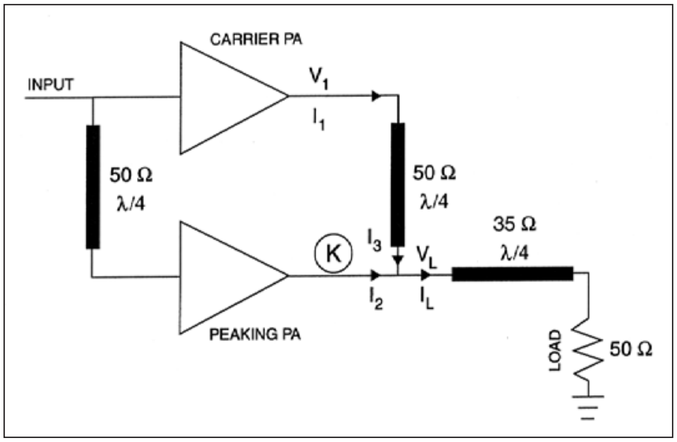

Figure 37 · Doherty transmitter.

the 25 ohms of the low-power region. Transformation through the quarter-wavelength line results in a decrease in the load presented to the carrier PA. The carrier PA remains in saturation and acts as a voltage source. It operates at peak efficiency, but delivers an increasing amount of power. At PEP output, both PAs see 50-ohm loads and each delivers half of the system output power. The PEP efficiency is that of the class-B PAs.

The resulting instantaneous-efficiency curve is shown in Figure 39. The classical power division (α = 0.5) approximately maximizes the average efficiency for full-carrier AM signals, as well as modern single-carrier digital signals. The use of other power-division ratios allows the lower efficiency peak to be shifted leftward so that the average efficiency is increased for signals with higher peak-to-average ratios. For example, α = 0.36 results in a 60 percent average efficiency for a Rayleigh-envelope signal with a 10-dB peak-to-average ratio, which is a factor of 2.1 improvement over class B. Doherty transmitters with unequal power division can be implemented by using different PEP load impedances and different supply voltages in the two PAs [97].

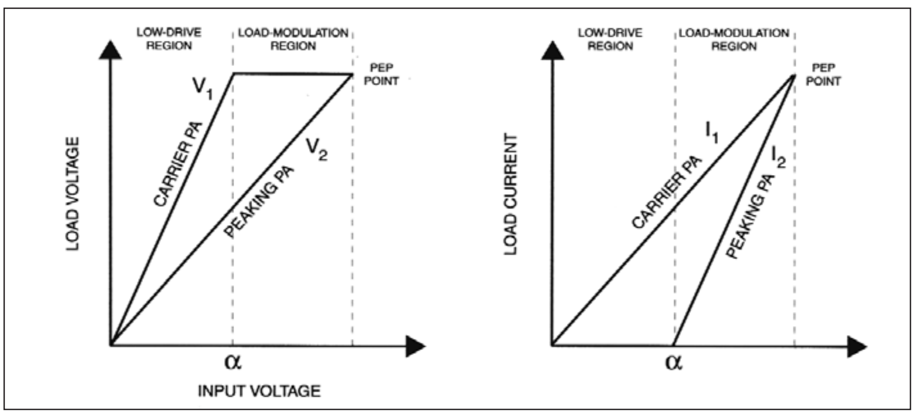

Figure 38 · Ideal voltage and current relationships in Doherty transmitter.

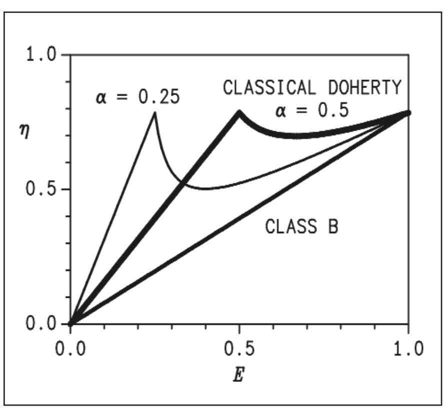

Figure 39 Instantaneous efficiency of the Doherty system with ideal class-B PAs.

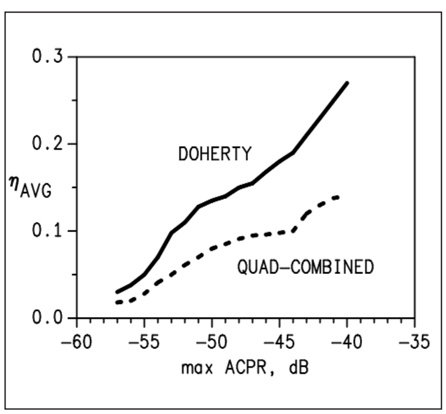

Figure 40 · Measured ACPR performance of an S-band Doherty transmitter.

Much recent effort has focused on accommodating non-ideal effects (e.g., nonlinearity, loss, phase shift) into a Doherty architecture [93, 94, 95]. The power consumed by the quiescent current of the peaking amplifier is also a concern. The measured ACPR characteristics of an S-band Doherty transmitter are compared to those of quadrature-combined class-B PAs in Figure 40. The signal is IS-95 forward link with pilot channel, paging channel, and sync-channel. The PAs are based upon 50-W LDMOS transistors. Back-off is varied to trade-off linearity against output. For the specified ACPR of –45 dBc, the average PAE is nearly twice that of the quadrature-combined PAs.

In a modern implementation, DSP can be used to control the drive and bias to the two PAs, for precise control and higher linearity. It is also possible to use three or more stages to keep the instantaneous efficiency relatively high over a larger dynamic range [96, 98]. For ideal class-B PAs, the average efficiency of a three-stage Doherty can be as high as 70 percent for a Rayleigh-envelope signal with 10-dB peak-to-average ratio.

References

60. S. C. Cripps, *RF Power Amplifiers for Wireless Communication,* Norwood, MA: Artech, 1999.

61. J. M. Rollett, “Stability and power-gain invariants of linear twoports,” *IRE Trans. Circuit Theory*, pp, 29-32, March 1962.

62. S. Cohn, “A class of broadband three-port TEM modes hybrids,” *IEEE Trans. Microwave Theory Tech.*, vol. MTT-

16, no. 2, pp. 110-116, 1968.

63. J. Goel, "K band GaAsFET amplifier with 8.2 W output using a radial power combiner," *IEEE Trans. Microwave Theory Tech.*, vol. MTT-32, no. 3, pp. 317-324, 1984.

64. A. Berr and D. Kaminsky, "The travelling wave power divider/combiner," *IEEE Trans. Microwave Theory Tech.*, vol. MTT-28, no.12, pp. 1468-1473, 1980.

65. F. H. Raab, "Hybrid and quadrature splitters and combiners," Research Note RN97-22, Green Mountain Radio Research Company, Colchester, VT, Sept. 20, 1997.

66. R. A. York and Z. B. Popovic, *Active and Quasi-Optical Arrays for Solid-State Power Combining*, New York: Wiley, 1997.

67. S. Brozovich, "High efficiency multiple power level amplifier circuit," U.S. Patent 5,661,434, Aug. 1997.

68. J. Sevic, "Efficient parallel stage amplifier," U.S. Patent 5,872,481, Feb. 1999.

69. F. H. Raab, "Average efficiency of Class-G power amplifiers," *IEEE Trans. Consumer Electronics*, vol. CE-32, no. 2, pp. 145-150, May 1986.

70. J. Staudinger, "Applying switched gain stage concepts to improve efficiency and linearity for mobile CDMA power amplification," *Microwave J.*, vol. 43, no. 9, pp. 152-162, Sept. 2000.

71. "30 way radial combiner for miniature GaAsFET power applications"

72. T. C. Choinski, "Unequal power division using several couplers to split and recombine the output," *IEEE Trans. Microwave Theory Tech.*, vol. MTT-32, no.6, pp. 613-620, 1984.

73. L. R. Kahn, "Single sideband transmission by envelope elimination and restoration," *Proc. IRE*, vol. 40, no. 7, pp. 803-806, July 1952.

74. F. H. Raab and D. J. Rupp, "High-efficiency single-sideband HF/VHF transmitter based upon envelope elimination and restoration," *Proc. Sixth Int. Conf. HF Radio Systems and Techniques* (HF '94) (IEE CP 392), York, UK, pp. 21-25, July 4 - 7, 1994.

75. F. H. Raab, B. E. Sigmon, R. G. Myers, and R. M. Jackson, "L-band transmitter using Kahn EER technique," *IEEE Trans. Microwave Theory Tech.*, pt. 2, vol. 46, no. 12, pp. 2220-2225, Dec. 1998.

76. F. H. Raab, "Intermodulation distortion in Kahn-technique transmitters," *IEEE Trans. Microwave Theory Tech.*, vol. 44, no. 12, part 1, pp. 2273-2278, Dec. 1996.

77. F. H. Raab, "Drive modulation in Kahn-technique transmitters," *Int. Microwave Symp. Digest*, vol. 2, pp. 811-814, Anaheim, CA, June 1999.

Acronyms Used in Part 3

EER	Envelope Elimination and Restoration
AM	Amplitude Modulation
LINC	Linear Amplification with Nonlinear Components

78. M. D. Weiss, F. H. Raab, and Z. B. Popovic, "Linearity characteristics of X-band power amplifiers in high-efficiency transmitters," *IEEE Trans. Microwave Theory Tech.*, vol. 47, no. 6, pp. 1174-1179, June 2001.

79. F. H. Raab, "Technique for wideband operation of power amplifiers and combiners," U. S. Patent 6,252,461, June 26, 2001.

80. J. Staudinger et al., "High efficiency CDMA RF power amplifier using dynamic envelope tracking technique," *Int. Microwave Symp. Digest*, vol. 2, pp. 873-876, Boston, MA, June 13-15, 2000.

81. A. A. M. Saleh and D. C. Cox, "Improving the power-added efficiency of FET amplifiers operating with varying-envelope signals," *IEEE Trans. Microwave Theory Tech.*, vol. 31, no. 1, pp. 51-55, Jan. 1983.

82. B. D. Geller, F. T. Assal, R. K. Gupta, and P. K. Cline, "A technique for the maintenance of FET power amplifier efficiency under backoff," *IEEE 1989 MTT-S Digest*, Long Beach, CA, pp. 949-952, June 1989.

83. G. Hanington, P.-F. Chen, P. M. Asbeck, and L. E. Larson, "High-efficiency power amplifier using dynamic power-supply voltage for CDMA applications," *IEEE Trans. Micro-wave Theory Tech.*, vol. 47, no. 8, pp. 1471-1476, Aug. 1999.

84. G. Hanington, A. Metzger, P. Asbeck, and H. Finlay, "Integrated dc-dc converter using GaAs HBT technology," *Electronics Letters*, vol. 35, no. 24, p.2110-2112, 1999.

85. D. R. Anderson and W. H. Cantrell, "High-efficiency inductor-coupled high-level modulator," *IMS '01 Digest*, Phoenix, AZ, May 2001.

86. H. Chireix, "High power outphasing modulation," *Proc. IRE*, vol. 23, no. 11, pp. 1370-1392, Nov. 1935.

87. D. C. Cox and R. P. Leck, "A VHF implementation of a LINC amplifier," *IEEE Trans. Commun.*, vol. COM-24, no. 9, pp. 1018-1022, Sept. 1976.

88. R. Langridge, T. Thornton, P. M. Asbeck, and L. E. Larson, "A power re-use technique for improving efficiency of outphasing microwave power amplifiers," *IEEE Trans. Microwave Theory Tech.*, vol. 47, no. 8, pp. 1467-1470 , Aug. 1999.

89. F. H. Raab, "Efficiency of outphasing power-amplifier systems," *IEEE Trans. Commun.*, vol. COM-33, no. 10, pp. 1094-1099, Oct. 1985.

90. B. Stengel and W. R. Eisenstat, "LINC power amplifier combiner efficiency optimization," *IEEE Trans. Veh. Technol.*, vol. 49, no. 1, pp. 229- 234, Jan. 2000.

91. C. P. Conradi, R. H. Johnston, and J. G. McRory, "Evaluation of a lossless combiner in a LINC transmitter," *Proc. 1999 IEEE Canadian Conf. Elec. and Comp. Engr.*, Edmonton, Alberta, Canada, pp. 105-109, May 1999.

92. W. H. Doherty, "A new high efficiency power amplifier for modulated waves," *Proc. IRE*, vol. 24, no. 9, pp. 1163-1182, Sept. 1936.

93. D. M. Upton and P. R. Maloney, "A new circuit topology to realize high efficiency, high linearity, and high power microwave amplifiers," *Proc. Radio and Wireless Conf.* (RAWCON), Colorado Springs, pp. 317-320, Aug. 9-12, 1998.

94. J. Schuss et al, "Linear amplifier for high efficiency multi-carrier performance," U.S. Patent 5,568,086, Oct. 1996.

95. J. Long, "Apparatus and method for amplifying a signal," U.S. Patent 5,886,575, March 1999.

96. F. H. Raab, "Efficiency of Doherty RF-power amplifier systems," *IEEE Trans. Broadcasting*, vol. BC-33, no. 3, pp. 77-83, Sept. 1987.

97. M. Iwamoto et al., "An extended Doherty amplifier with high efficiency over a wide power range," *Int. Microwave Symp. Digest*, Phoenix, AZ, pp. 931-934, May 2001.

98. B. E. Sigmon, "Multistage high efficiency amplifier," U.S. Patent 5,786,938, July 28, 1998.

Author Information

The authors of this series of articles are: Frederick H. Raab (lead author), Green Mountain Radio Research, e-mail: f.raab@ieee.org; Peter Asbeck, University of California at San Diego; Steve Cripps, Hywave Associates; Peter B. Kenington, Andrew Corporation; Zoya B. Popovic, University of Colorado; Nick Pothecary, Consultant; John F. Sevic, California Eastern Laboratories; and Nathan O. Sokal, Design Automation. Readers desiring more information should contact the lead author.

RF and Microwave Power Amplifier and Transmitter Technologies — *Part 4*

By Frederick H. Raab, Peter Asbeck, Steve Cripps, Peter B. Kenington, Zoya B. Popovich, Nick Pothecary, John F. Sevic and Nathan O. Sokal

Linearization methods are the focus of Part 4 of our series on power amplifiers, which describes the basic architecture and performance capabilities of feedback, feedforward and predistortion techniques

Linearization techniques are incorporated into power amplifiers and transmitters for the dual purposes of improving linearity and for allowing operation with less back-off and therefore higher efficiency. This article provides a summary of the three main families of techniques have been developed: Feedback, feedforward, and predistortion.

8a. FEEDBACK

Feedback linearization can be applied either directly around the RF amplifier (RF feedback) or indirectly upon the modulation (envelope, phase, or I and Q components).

RF Feedback

The basis of this technique is similar to its audio-frequency counterpart. A portion of the RF-output signal from the amplifier is fed back to, and subtracted from, the RF-input signal without detection or down- conversion. Considerable care must be taken when using feedback at RF as the delays involved must be small to ensure stability. In addition, the loss of gain at RF is generally a more significant sacrifice than it is at audio frequencies. For these reasons, the use of RF feedback in discrete circuits is usually restricted to HF and lower VHF frequencies [99]. It can be applied within MMIC devices, however, well into the microwave region.

In an active RF feedback system, the voltage divider of a conventional passive-feedback system is replaced by an active (amplifier) stage. The gain in the feedback path reduces the power dissipated in the feedback components. While such systems demonstrate IMD reduction [105], they tend to work best at a specific signal level.

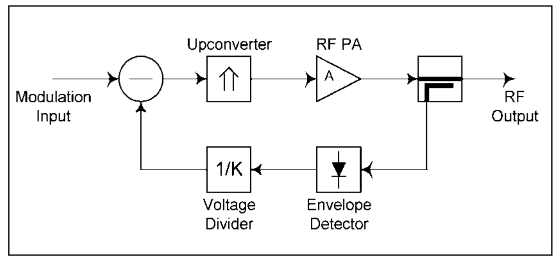

Fig 41 · Envelope feedback applied to a complete transmitter.

Envelope Feedback

The problem of delay in RF feedback is alleviated to a large extent by utilizing the signal envelope as the feedback parameter. This approach takes care of in-band distortion products associated with amplitude nonlinearity. Harmonic distortion products, which are corrected by RF feedback, are generally not an issue as they can easily be removed by filtering in most applications. Envelope feedback is therefore a popular and simple technique.

Envelope feedback can be applied to either a complete transmitter (Figure 41) or a single power amplifier (Figure 42). The principles of operation are similar and both are described in detail in [100]. The RF input signal is sampled by a coupler and the envelope of the input sample is detected. The resulting envelope is then fed to one input of a differential amplifier, which subtracts it from a similarly

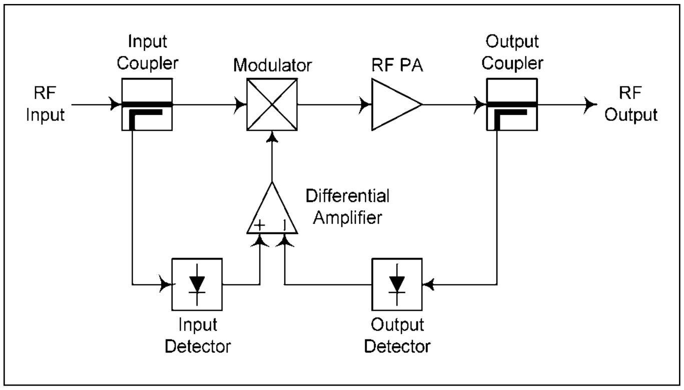

Figure 42 · Envelope feedback applied to an RF power amplifier.

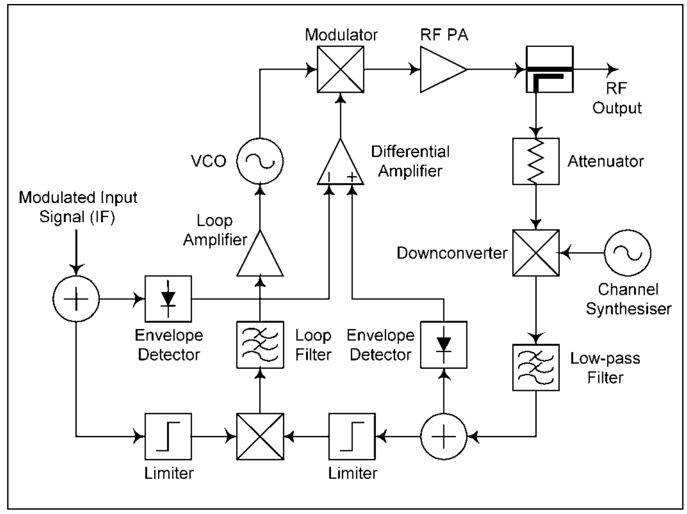

Figure 43 · Block diagram of a polar-loop transmitter.

obtained sample of the RF output. The difference signal, representing the error between the input and output envelopes, is used to drive a modulator in the main RF path. This modulator modifies the envelope of the RF signal which drives the RF PA. The envelope of the resulting output signal is therefore linearized to a degree determined by the loop gain of the feedback process. Examples of this type of system are reported in [101] and [102].

The degree of linearity improvement that can be obtained when using this technique depends upon the relative levels of the AM-AM and AM-PM conversion in the amplifier. For a VHF BJT amplifier, AM-AM distortion is dominant and two-tone IMD is typically reduced by 10 dB. Since AM-PM distortion is not corrected by envelope feedback, no linearity improvement is observed if phase distortion is the dominant form of nonlinearity. This is often the case in, for example, class-C and LDMOS PAs. The use of envelope feedback is therefore generally restricted to relatively linear class-A or AB amplifiers.

Polar-Loop Feedback

The polar-loop technique overcomes the fundamental inability of envelope feedback to correct for AM-PM distortion effects [103]. Essentially, a phase-locked loop is added to the envelope feedback system as shown in Figure 43. For a narrowband VHF PA, the improvement in two-tone IMD is typically around 30 dB.

The envelope- and phase-feedback functions operate essentially independently. In this case, envelope detection occurs at the intermediate frequency (IF), as the input signal is assumed to be a modulated carrier at IF. Likewise, phase detection takes place at the IF, with limiting being used to minimize the effects of signal amplitude upon the detected phase. Alternatively, it is possible to supply the envelope and phase modulating signals separately at baseband and to undertake the comparisons there.

The key disadvantage of polar feedback lies in the generally different bandwidths required for the amplitude and phase feedback paths. Thus, differing levels of improvement of the AM-AM and AM-PM characteristics usually result, and this often leads to a poorer overall performance than that achievable from an equivalent Cartesian-loop transmitter. A good example of the difference occurs with a standard two-tone test, which causes the phase-feedback path to cope with a discontinuity at the envelope minima. In general, the phase bandwidth must be five to ten times the envelope bandwidth, which limits available loop gain for a given delay.

Cartesian Feedback

The Cartesian-feedback technique overcomes the problems associated with the wide bandwidth of the signal phase by applying modulation feedback in I and Q (Cartesian) components [104]. Since the I and Q components are the natural outputs of a modern DSP, the Cartesian loop is widely used in PMR and SMR systems.

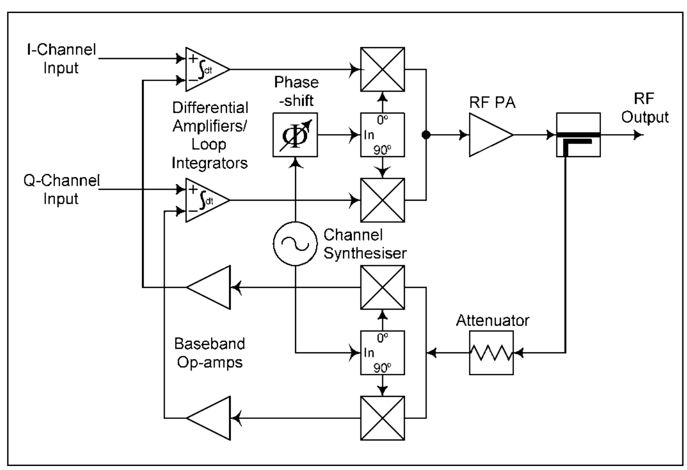

Figure 44 · Cartesian-loop transmitter configuration.

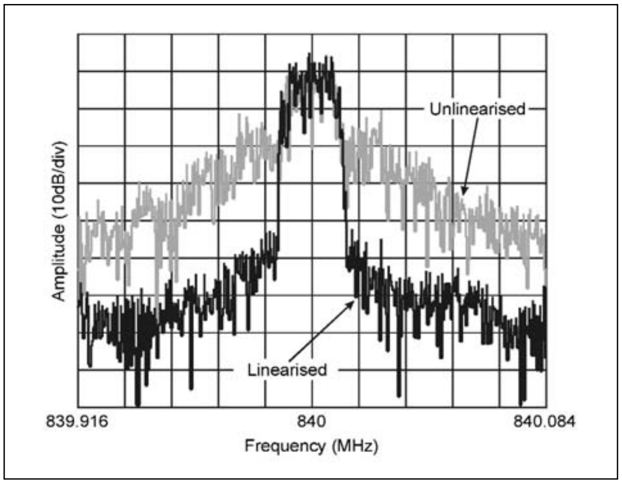

Figure 45 · Linearization of a class-C PA by Cartesian feedback (courtesy WSI).

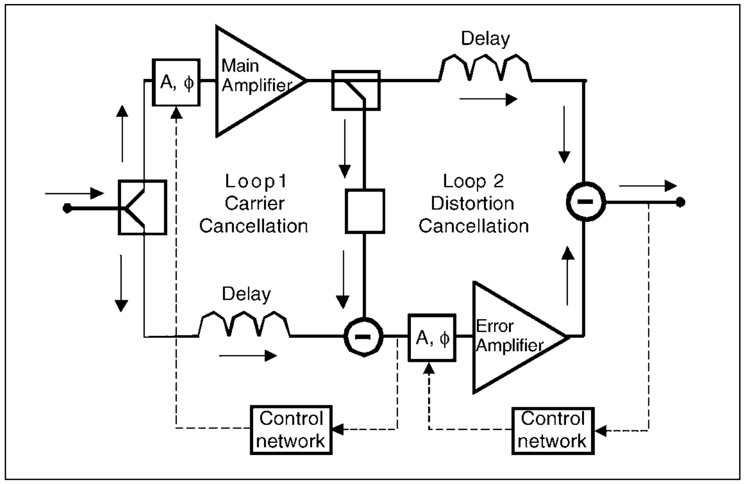

Figure 46 · Block diagram of a feed-forward transmitter in its basic form.

The basic Cartesian loop (Figure 44) consists of two identical feedback processes operating independently on the I and Q channels. The inputs are applied to differential integrators (in the case of a first-order loop) with the resulting difference (error) signals being modulated onto I and Q subcarriers and up-converted to drive the PA. A sample of the output from the PA is attenuated and quadrature-down-converted (synchronously with the up-conversion process). The resulting quadrature feedback signals then form the second inputs to the input differential integrators, completing the two feedback loops. The phase shifter shown in the up-converter local-oscillator path is used to align the phases of the up- and down-conversion processes, thereby ensuring that a negative feedback system is created and that the phase margin of the system is optimized.

The effects of applying Cartesian feedback to a highly nonlinear (class-C) PA amplifying an IS-136 (DAMPS) signal are shown in Figure 45. The first ACPR is improved by 35 dB and the signal is produced within specifications with an efficiency of 60 percent [100].

8b. FEEDFORWARD

The very wide bandwidths (10 to 100 MHz) required in multicarrier applications can render feedback and DSP impractical. In such cases, the feedforward technique can be used to achieve ultra-linear operation. In its basic configuration, feedforward typically gives improvements in distortion ranging from 20 to 40 dB.

Operation

In its basic form (Figure 46), a feedforward amplifier consists of two amplifiers (the main and error amplifiers), directional couplers, delay lines and loop control networks [110]. The directional couplers are used for power splitting/combining, and the delay lines ensure operation over a wide bandwidth. Loop-control networks, which consist of amplitude- and phase-shifting networks, maintain signal and distortion cancellation within the various feedforward loops.

The input signal is first split into two paths, with one path going to the high-power main amplifier while the other signal path goes to a delay element. The output signal from the main amplifier contains both the desired signal and distortion. This signal is sampled and scaled using attenuators before being combined with the delayed portion of the input signal, which is regarded as distortion-free. The resulting “error signal” ideally contains only the distortion components in the output of the main amplifier. The error signal is then amplified by the low-power, high-linearity error amplifier, and then combined with a delayed version of the main amplifier output. This second combination ideally cancels the distortion components in the main-amplifier output while leaving the desired signal unaltered.

In practice, there is always some residual desired signal passing through the error amplifier. This is in general not a problem unless the additional power is sufficient in magnitude to degrade the linearity of the error amplifier and hence the linearity of the feedforward transmitter.

Signal Cancellation

Successful isolation of an error signal and the removal of distortion components depend upon precise signal cancellation over a band of frequencies. In practice, cancellation is achieved by the vector addition of signal voltages. The allowable amplitude and phase mismatches for different cancellation levels are shown in Figure 47. For manufactured equipment, realistic values of distortion

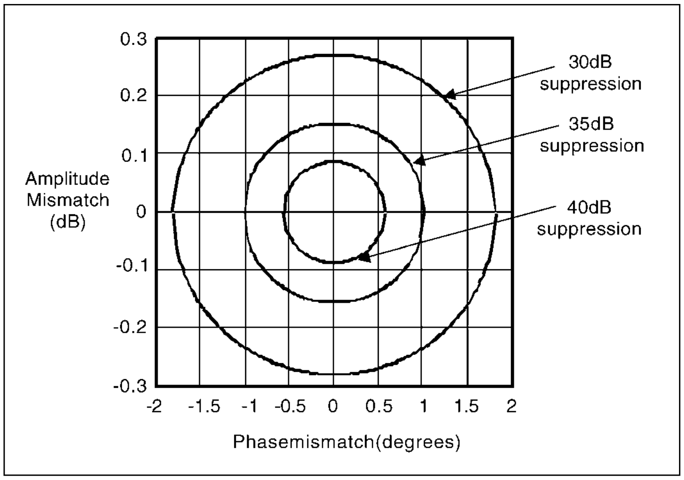

Figure 47 · Gain/phase matching requirements.

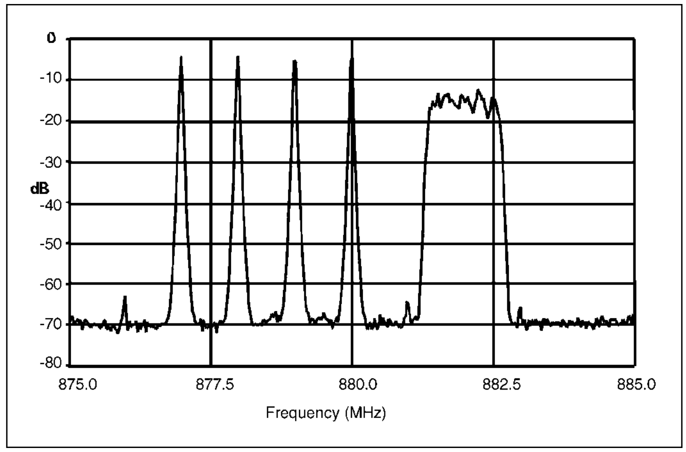

Figure 48 · Feedforward performance with mixed-mode modulation (TDMA and CDMA signals).

cancellation are around 25 to 30. The limiting factor is nearly always the bandwidth over which a given accuracy can be obtained.

Efficiency

The outputs of the main and error amplifiers are typically combined in a directional coupler that both isolates the PAs from each other and provides resistive input impedances. For a typical 10 dB coupling ratio, 90 percent of the power from the main PA reaches the output. For the same coupling ratio, only 10 percent of the power from the error amplifier reaches the load, thus the error amplifier must produce ten times the power of the distortion in the main amplifier. The peak-to-average ratio of the error signal is often much higher than that of the desired signal, making amplification of the error signal inherently much less efficient than that of the main signal. As a result, the power consumed by the error amplifier can be a significant fraction (e.g., one third) of that of the main amplifier. In addition, it may be necessary to operate one or both amplifiers well into back-off to improve linearity. The overall average efficiency of a feedforward transmitter may therefore be only 10 to 15 percent for typical multi-carrier signals.

Automatic Loop Control

Since feedforward is inherently an open-loop process, changes in device characteristics over time, temperature, voltage and signal level degrade the amplitude and phase matching and therefore increase distortion in the transmitter output. An automatic control scheme continuously adjusts the gain and phase to achieve the best signal cancellation and output linearity. The first step is to use FFT techniques, direct power measurement, or pilot signals to determine how well the loop is balanced. Both digital and analog techniques can be used for loop control and adjustment. Signal processing can be used to reduce the peaks in multi-carrier signals and to keep distortion products out of the nearby receiving band [111].

Performance

An example of the use of feedforward to improve linearity is shown in Figure 48. The signal consists of a mix of TDMA and CDMA carriers. The power amplifiers are based upon LDMOS transistors and have two-tone IMD levels in the range –30 to –35 dBc at nominal output power. The addition of feedforward reduces the level of distortion by approximately 30 dB to meet the required levels of better than –60 dBc. The average efficiency is typically about 10 percent.

8c. PREDISTORTION

The basic concept of a predistortion system (Figure 49) involves the insertion of a nonlinear element prior to the

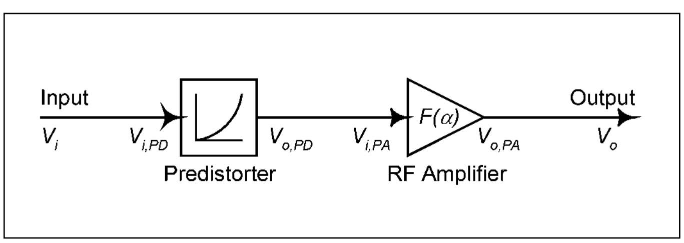

Figure 49 · Predistortion concept.

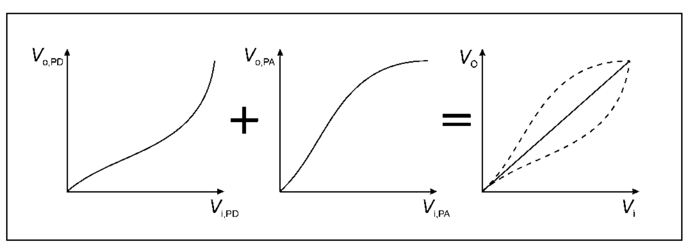

Figure 50 · Amplitude correction by predistortion.

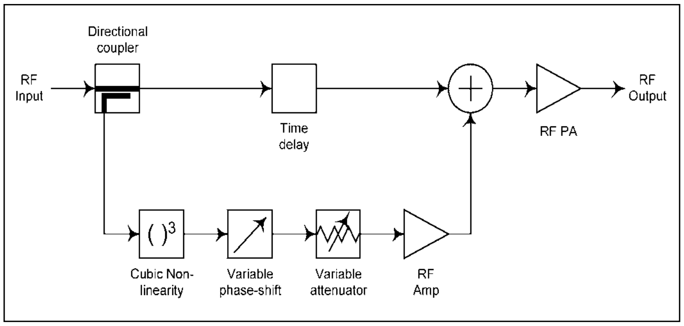

Figure 51 · An RF predistorter.

RF PA such that the combined transfer characteristic of both is linear (Figure 50). Predistortion can be accomplished at either RF or baseband.

RF Predistortion

The block diagram of a simple RF predistorter is shown in Figure 51. A compressive characteristic, created by the nonlinearity in the lower path (e.g., a diode) is subtracted from a linear characteristic (the upper path) to generate an expansive characteristic. The output of the linear path (typically just a time delay) is given by:

$$v_l(v_{in}) = a_1 v_{in} \tag{1}$$

and that of the compressive path is given by

$$v_c(v_{in}) = a_2 v_{in} - b v_{in}^3 \tag{2}$$

Subtracting the above equations gives

$$v_{pd}(v_{in}) = (a_2 - a_2) v_{in} - b v_{in}^3 \tag{3}$$

This is now an expansive characteristic with a linear gain of $a_1 - a_2$, and may be used to predistort a compressive amplifier characteristic (cubic in this example) by appropriate choice of a_1, a_2 and b.

An example of the results from using a simple diode-based RF predistorter with a 120-W LDMOS PA amplifying an IS-95 CDMA signal is shown Figure 52. When applied to π/4-DQPSK modulation in a satellite application, the same predistorter roughly halves the EVM, improves the efficiency from 22 to 29 percent, and doubles the available output power.

Predistortion bandwidths tend to be limited by similar factors to that of feedforward, namely gain and phase flatness of the predistorter itself and of the RF PA. In addition, memory effects in the PA and the predistorter limit the degree cancellation, and these tend to become poorer with increasing bandwidth.

Better performance can be achieved with more complex forms of RF predistortion such as Adaptive Parametric Linearization (APL®), which is capable of multi-order correction [106]. Most RF-predistortion techniques are capable of broadband operation with practical operational bandwidths similar to, or greater than, those of feedforward.

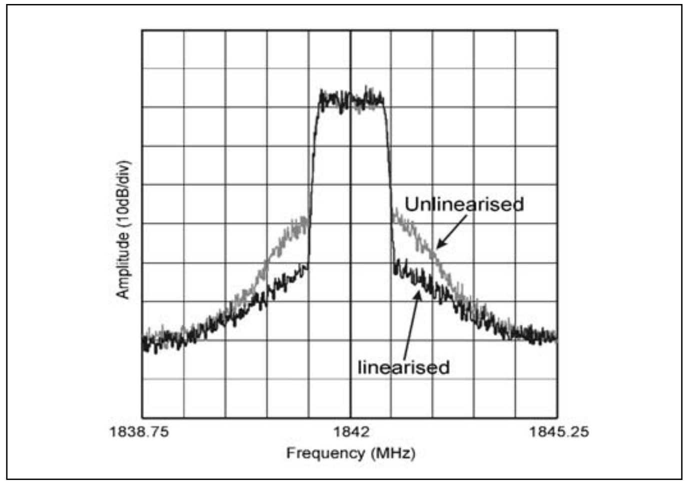

Figure 52 · Linearization by diode-based RF predistorter (courtesy WSI).

Digital Predistortion

Digital predistortion techniques exploit the considerable processing power now available from DSP devices, which allows them both to form and to update the required predistortion characteristic. They can operate with analog-baseband, digital-baseband, analog-IF, digital-IF, or analog-RF input signals. Digital-baseband and digital-IF processing are most common.

The two most common types of digital predistorter are termed mapping predistorters [107] and constant-gain

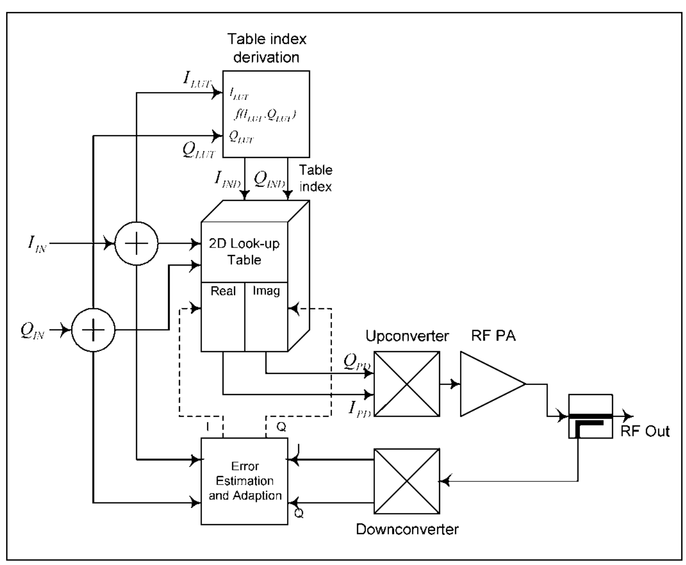

Figure 53 · Mapping predistorter.

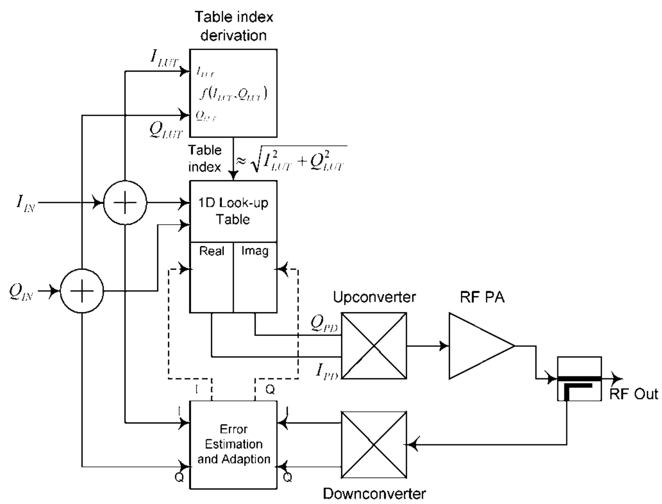

Figure 54 · Constant-gain predistorter.

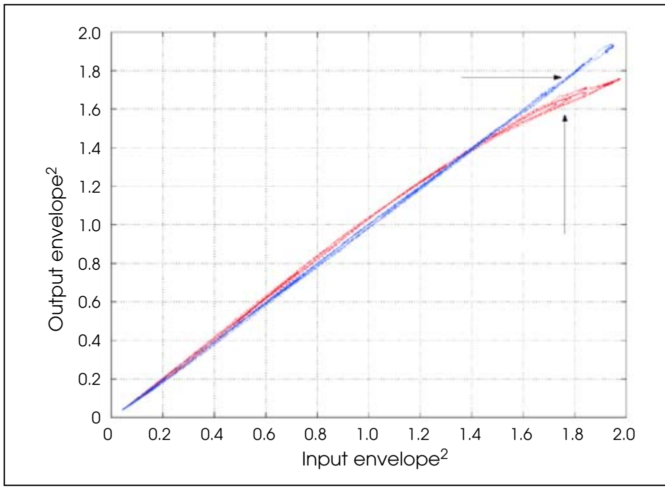

Figure 55 · Linearization of the amplitude transfer characteristic using an RF input/output digital predistorter (courtesy WSI).

predistorters [108]. A mapping predistorter utilizes two look-up tables, each of which is a function of two variables (I_{IN} and Q_{IN}), as shown in Figure 53. This type of predistorter is capable of excellent performance. However, it requires a significant storage and/or processing overhead for the look-up tables and their updating mechanism, and has a low speed of convergence. The low convergence speed results from the need to address all points in the I/Q complex plane before convergence can be completed.

A constant-gain predistorter (Figure 54) requires only a single-dimensional look-up table, indexed by the signal envelope. It is therefore a much simpler implementation and requires significantly less memory for a given level of performance and adaptation time. It uses the look-up table to force the predistorter and associated PA to exhibit a constant gain and phase at all envelope levels. The overall transfer characteristic is then linear:

$$G_{PD}(I_{IN}(t),Q_{IN}(t))\times G_{PA}(I_{PD}(t),Q_{PD}(t)) = k \qquad (4)$$

An example of the improvement in the amplitude-transfer characteristic by an RF-input/output digital predistorter [109] is shown in Figure 55. The plot is based upon real-time using samples from a GSM-EDGE signal. Both the gain expansion and compression are improved by the linearizer. EVM is reduced from around 4.5 to 0.7 percent. The ACPR for IS-136 DAMPS modulation (π/4-DQPSK) is reduced by nearly 20 dB (Figure 56). When generating mask-compliant EDGE modulation at full output power (850-900 MHz), the linearized PA has an efficiency of over 30 percent.

An example of linearization of a PA with two 3G W-

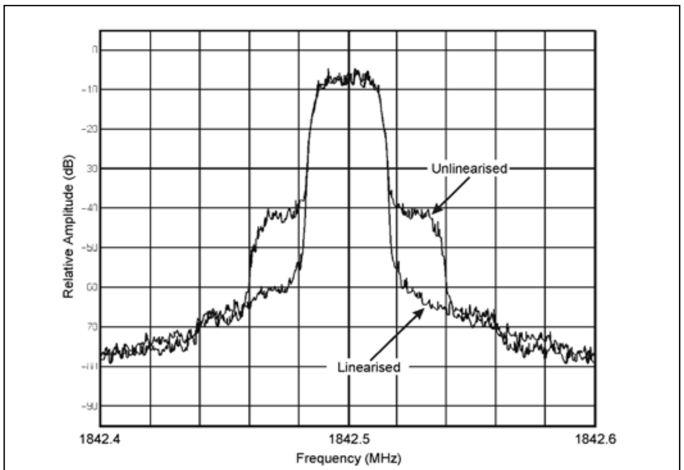

Figure 56 · Linearization of DAMPS PA by RF input/output predistorter (courtesy WSI).

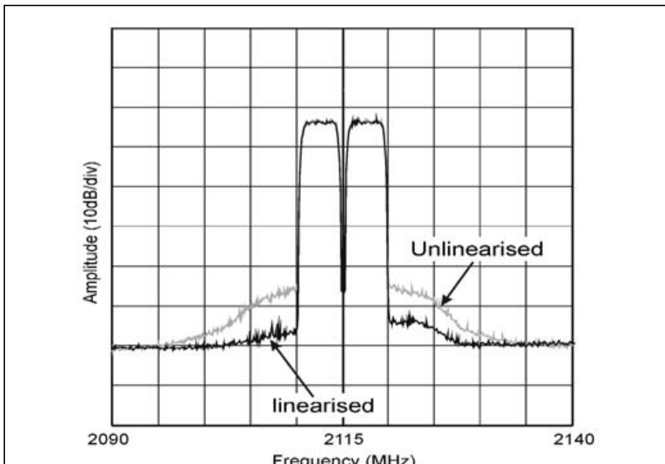

Figure 57 · Linearization of 3G W-CDMA PA signal by digitial baseband input predistorter (courtesy WSI).

Figure 58 · A multi-carrier S-band transmitter with digital predistorter (courtesy WSI).

CDMA signals by a digital baseband-input predistorter is shown in Figure 57. The linearized amplifier meets the required spectral mask with a comfortable margin at all frequency offsets. The noise floor is set by the degree of clipping employed on the waveform, which limits the ACPR improvement obtained. It clearly demonstrates, however, that digital predistortion can be used in broadband as well as narrowband applications. Figure 58 shows a 3G transmitter that uses digital predistortion.

References

99. A. F. Mitchell, "A 135 MHz feedback amplifier," *IEE Colloq. Broadband High Frequency Amplifiers: Practice and Theory*, pp. 2/1-2/6, London, Nov. 22, 1979

100. P. B. Kenington, *High Linearity RF Amplifier Design,* Norwood, MA: Artech, 2000.

101. W. B. Bruene, "Distortion reducing means for single-sidedband transmitters," *Proc. IRE*, vol. 44, no. 12, pp. 1760-1765, Dec. 1956.

102. T. Arthanayake and H. B. Wood, "Linear amplification using envelope feedback," *Electronics Letters*, vol. 7, no. 7, pp. 145-146, April 8, 1971.

103. V. Petrovic and W. Gosling, "Polar-loop transmitter," *Electronics Letters*, vol. 15, no. 10, pp. 286-287, May 10, 1979.

104. V. Petrovic, "Reduction of spurious emission from radio transmitters by means of modulation feedback," *Proc. IEE Conf. No. 224 on Radio Spectrum Conservation Techniques*, UK., Sept. 6-8 1983.

105. E. Ballesteros, F. Perez, and J. Peres, "Analysis and design of microwave linearized amplifiers using active feedback," *IEEE Trans. Microwave Theory Tech.*, vol. 36, no. 3, pp. 499-504, March 1988.

106. P. B. Kenington, "Achieving high-efficiency in multi-carrier base-station power amplifiers," *Microwave Engr. Europe*, pp. 83-90. Sept. 1999.

107. Y. Nagata, "Linear amplification techniques for digital mobile communications," *Proc. IEEE Veh. Tech. Conf.* (VTC '89), San Fransisco, pp. 159-164, May 1-3, 1989.

108. J. K. Cavers, "Amplifier linearisation using a digital predistorter with fast adaptation and low memory requirements," *IEEE Trans. Veh. Tech.*, vol. 39, no. 4, pp. 374-382, Nov. 1990.

109. P. B. Kenington, M. Cope, R. M. Bennett, and J. Bishop, "GSM-EDGE high power amplifier utilising digital linearisation," *IMS'01 Digest*, Phoenix, AZ, May 20-25, 2001.

110. N. Pothecary, *Feedforward Linear Power Amplifiers*, Norwood, MA: Artech, 1999.

111. J. Tellado, *Multicarrier Modulation with Low PAR*, Boston: Kluwer, 2000.

Author Information

The authors of this series of articles are: Frederick H. Raab (lead author), Green Mountain Radio Research, e-mail: f.raab@ieee.org; Peter Asbeck, University of California at San Diego; Steve Cripps, Hywave Associates; Peter B. Kenington, Andrew Corporation; Zoya B. Popovic, University of Colorado; Nick Pothecary, Consultant; John F. Sevic, California Eastern Laboratories; and Nathan O. Sokal, Design Automation. Readers desiring more information should contact the lead author.

Acronyms Used in Part 4

ACPR	Adjacent Channel Power Ratio
APL	Adaptive Parametric Linearization
BER	Bit Error Rate
DAMPS	Digital American Mobile Phone System
EDGE	Enhanced Data for GSM Evolution
EVM	Error Vector Magnitude
IF	Intermediate Frequency
LDMOS	Laterally Diffused Metal Oxide Semiconductor
PA	Power Amplifier
PDF	Probability-Density Function
PMR	Private Mobile Radio
SMR	Specialized Mobile Radio
W-CDMA	Wideband Code-Division Multiple Access

From January 2004 *High Frequency Electronics*

RF and Microwave Power Amplifier and Transmitter Technologies — *Part 5*

By Frederick H. Raab, Peter Asbeck, Steve Cripps, Peter B. Kenington, Zoya B. Popovich, Nick Pothecary, John F. Sevic and Nathan O. Sokal

Emerging techniques are examined in this final installment of our series on power amplifier technologies, providing notes on new modulation methods and improvements in linearity and efficiency

The ever-increasing demands for more bandwidth, coupled with requirements for both high linearity and high efficiency create ever-increasing challenges in the design of power amplifiers and transmitters. A single W-CDMA signal, for example, taxes the capabilities of a Kahn-technique transmitter with a conventional class-S modulator. More acute are the problems in base-station and satellite transmitters, where multiple carriers must be amplified simultaneously, resulting in peak-to-average ratios of 10 to 13 dB and bandwidths of 30 to 100 MHz.

A number of the previously discussed techniques can be applied to this problem, including the Kahn EER with class-G modulator or split-band modulator, Chireix outphasing, and Doherty. This section presents some emerging technologies that may be applied to wideband, high efficiency amplification in the near future.

RF Pulse-Width Modulation

Variation of the duty ratio (pulse width) of a class-D RF PA [112] produces an amplitude-modulated carrier (Figure 59). The output envelope is proportional to the sine of the pulse width, hence the pulse width is varied in proportion to the inverse sine of the desired envelope. This can be accomplished in DSP, or by comparison of the desired envelope to a full-wave rectified sinusoid. The pulse timing conveys signal phase information as in the Kahn and other techniques.

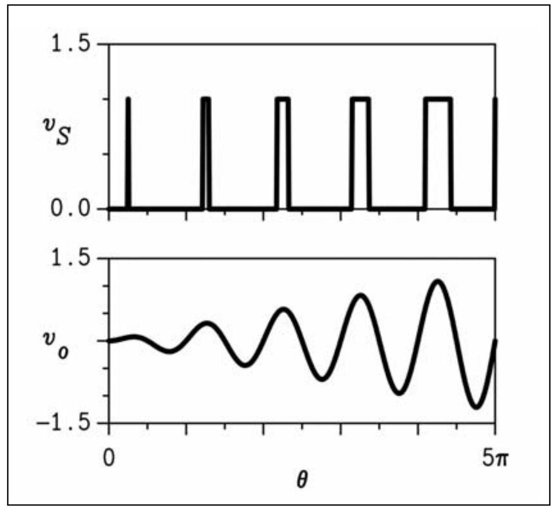

Figure 59 · RF pulse-width modulation.

Radio-frequency pulse-width modulation (RF PWM) eliminates the series-pass losses associated with the class-S modulator in a Kahn-technique transmitter. More importantly, the spurious products associated with PWM are located in the vicinity of the harmonics of the carrier [113] and therefore easily removed. Consequently, RF PWM can accommodate a significant RF bandwidth with only a simple, low-loss output filter.

Ideally, the efficiency is 100 percent. In practice, switching losses are increased over those in a class-D PA with a 50:50 duty ratio because drain current is nonzero during switching.

This series of articles is an expanded version of the paper, "Power Amplifiers and Transmitters for RF and Microwave" by the same authors, which appeared in the the 50th anniversary issue of the *IEEE Transactions on Microwave Theory and Techniques*, March 2002. © 2002 IEEE. Reprinted with permission.

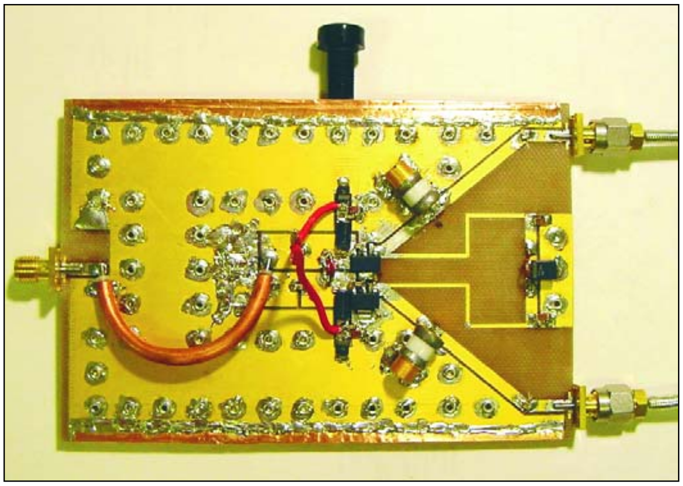

Figure 60 · Current-switching PA for 1 GHz (courtesy UCSD).

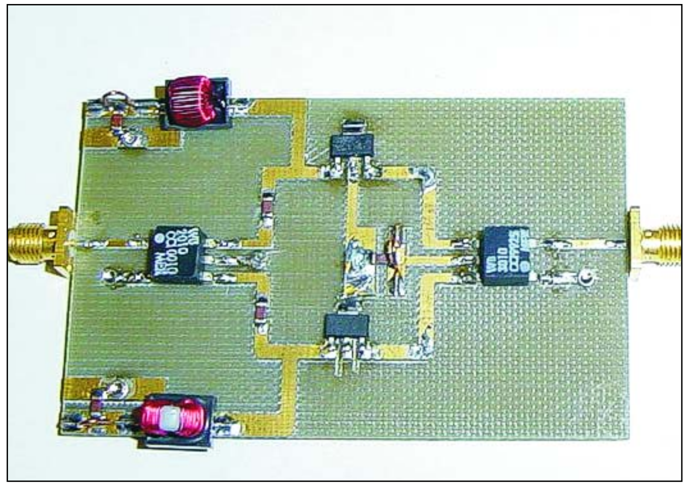

Figure 61 · Prototype class-D PA for delta-sigma modulation (courtesy UCSD).

Previous applications of RF PWM have been limited to LF and MF transmitters (e.g., GWEN [114]). However, the recent development of class-D PAs for UHF and microwave frequencies (Figure 60) offers some interesting possibilities.

Delta-Sigma Modulation

Delta-sigma modulation is an alternative technique for directly modulating the carrier produced by a class-D RF PA (Figure 61) [PA8],[PA9]. In contrast to the basically analog operation of RF PWM, delta-sigma modulation drives the class-D PA at a fixed clock rate (hence fixed pulse width) that is generally higher than the carrier frequency (Figure 62). The polarity of the drive is toggled as necessary to create the desired output envelope from the average of the cycles in the PA. Phase is again conveyed in pulse timing.

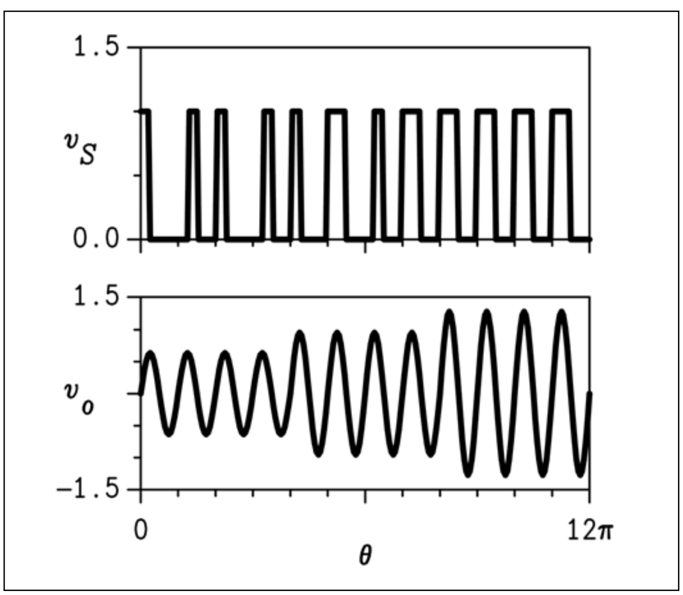

Figure 62 · Delta-sigma modulation.

The delta-sigma modulator employs an algorithm such as that shown in Figure 63. The signal is digitized by a quantizer (typically a single-bit comparator) whose output is subtracted from the input signal through a digital feedback loop, which acts as a band-pass filter. Basically, the output signal in the pass band is forced to track the desired input signal. The quantizing noise (associated with the averaging process necessary to obtain the desired instantaneous output amplitude) is forced outside of the pass band.

The degree of suppression of the quantization noise depends on the oversampling ratio; i.e., the ratio of the digital clock frequency to the RF bandwidth and is relatively independent of the RF center frequency. An example of the resultant spectrum for a single 900-MHz carrier and 3.6-GHz clock is shown in Figure 64. The quantization noise is reduced over a bandwidth of 50 MHz, which is sufficient for the entire cellular band. Out-of-band noise increases gradually and must be removed by a band-pass filter with sufficiently steep skirts.

As with RF PWM, the efficiency of a practical delta-sigma modulated class-D PA is reduced by switching losses associated with nonzero current at the times of switching. The narrow-band output filter may also introduce significant loss.

Carrier Pulse-Width Modulation

Carrier pulse-width modulation was first used in a UHF rescue radio at Cincinnati Electronics in the early 1970s. Basically, pulse-width modulation as in a class-S modulator gates the RF drive (hence RF drain current) on and off in bursts, as shown in Figure 65. The width of each burst is proportional to the instantaneous envelope of the

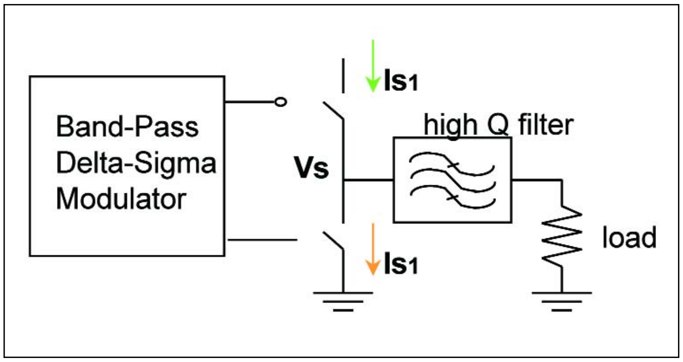

Figure 63 · Delta-sigma modulator.

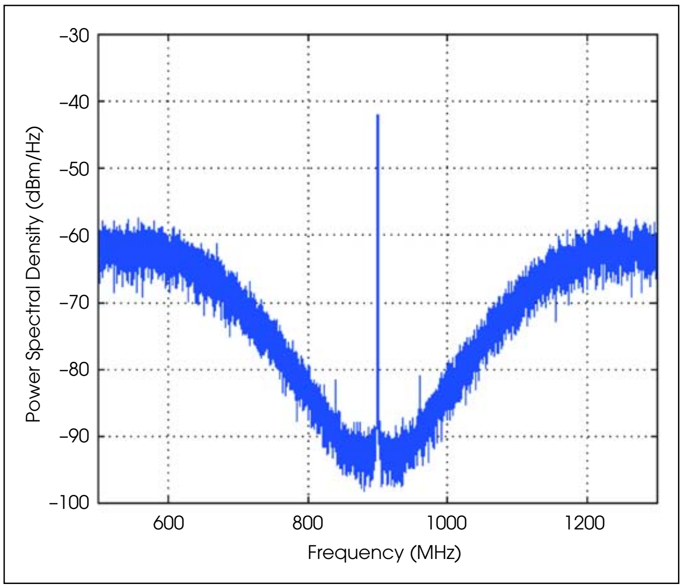

Figure 64 · Spectrum of delta-sigma modulation.

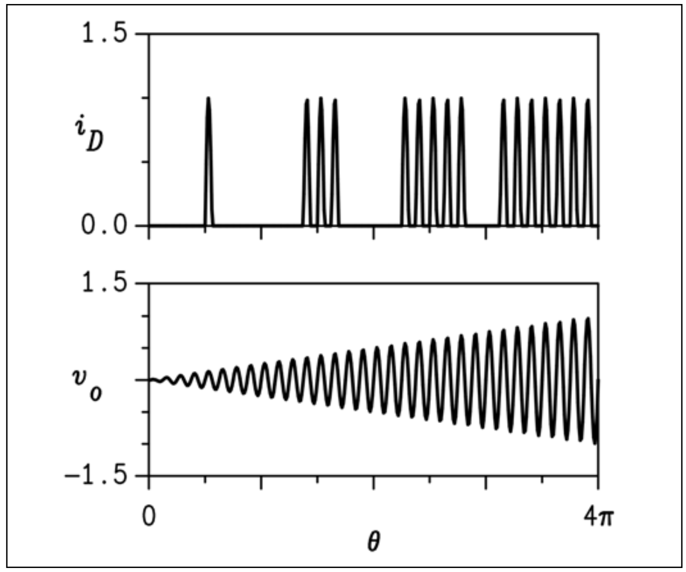

Figure 65 · Carrier pulse-width modulation.

desired output. The amplitude-modulated output signal is recovered by a band-pass filter that removes the sidebands associated with the PWM switching frequency. The PWM signal can be generated by a comparator as in a class-S modulator or by delta-sigma techniques.

As with RF PWM and delta-sigma modulation, the series-pass losses and bandwidth limitations of the high-level modulator are eliminated. The switching frequency in carrier PWM is not limited by capabilities of power-switching devices and can therefore easily be tens of MHz, allowing large RF bandwidths. A second advantage is that carrier PWM can be applied to almost any type of RF PA. A disadvantage is that a narrow-band output filter with steep skirts is required to remove the switching-frequency sidebands, and such filters tend to have losses of 1 to 2 dB at microwave frequencies. Nonetheless, the losses in the filter may be more than offset by the improvement in efficiency for signals with high peak-to-average ratios.

Power Recovery

A number of RF processes result in significant RF power dissipated in "dump" resistors. Examples include power reflected from a mismatched load and dumped by a circulator and the difference between two inputs of hybrid combiner dumped to the balancing resistor. The notion of recovering and reusing wasted RF power was originally applied to the harmonics (18 percent of the output power) of an untuned LF class-D PA [117].

More recently, power recovery has been applied to outphasing PAs with hybrid combiners [118, 119]. The instantaneous efficiency of such a system depends upon both the efficiency of the PA and that of the recovery system. Since the two PAs operate at full power regardless of the system output, inefficiency in the PA has a significant impact upon the system efficiency at the lower outputs. Nonetheless, a significant improvement over conventional hybrid-coupled outphasing is possible, and the PAs are presented with resistive loads that allow them to operate optimally. Typically, 50 percent of the dumped power can be recovered.

The power-recovery technology can also be used to implement miniature DC-DC converters. Basically, a high-efficiency RF-power amplifier (e.g., class-E) converts DC to RF and a high-efficiency rectifier circuit converts the RF to DC at the desired voltage. Implementation at microwave frequencies reduces the size of the tuning and filtering components, resulting in a very small physical size and high power density. In a prototype that operates at C band [120], the class-E PA uses a single MESFET to produce 120 mW with a PAE of 86 percent. The diode rectifier consists of a directional coupler with two Schottky

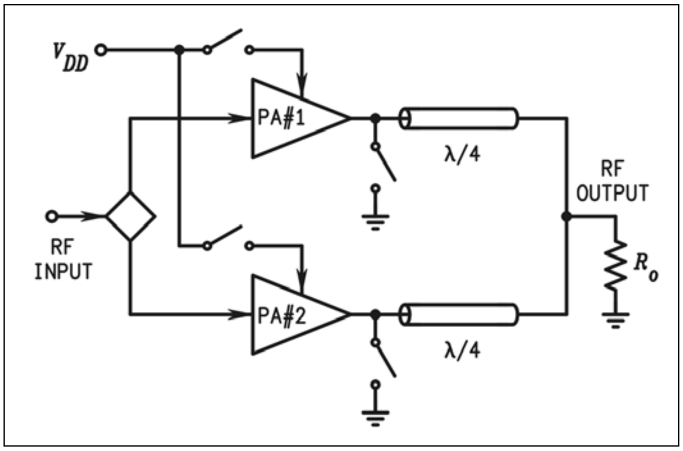

Figure 66 · Switched PAs with quarter-wavelength transmission line combiner.

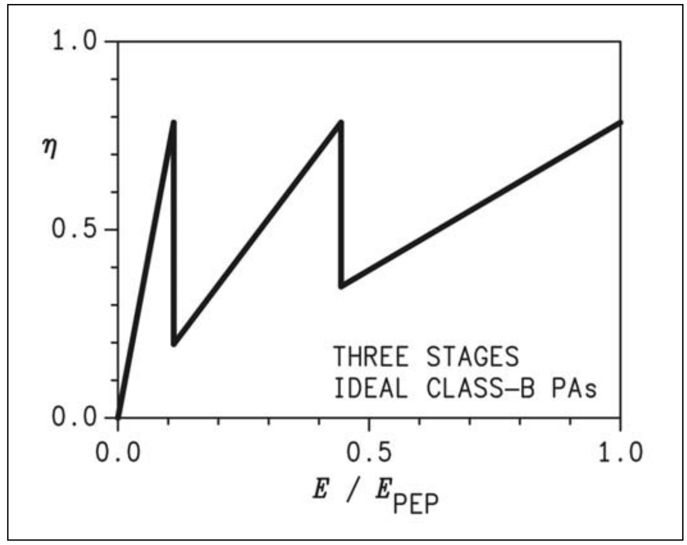

Figure 67 · Instantaneous efficiency of switched PAs.

diodes connected at the coupled and through ports and has a 98-percent conversion efficiency and an overall efficiency (including mismatch loss) of 83 percent. For a typical DC output of 3 V, the DC-DC conversion efficiency is 64 percent.

Switched PAs with Transmission-Line Combiners

RF-power amplifiers cannot simply be connected in series or parallel and switched on and off to make a transmitter module that adapts to variable peak envelope power. Attempting to do so generally produces either little effect or erratic variations in load impedance, sometimes leading to unstable operation and destruction of the transistors. Systems of microwave PAs that are toggled on and off are therefore connected through networks of quarter-wavelength transmission lines. The Doherty transmitter (discussed in part 4 of this series) is a classic example of this sort of technique.

An alternative topology (Figure 66) uses shorting switches and quarter-wavelength lines to to decouple off-state PAs [121, 122]. The inactive PA is powered-down (by switching off its supply voltage), after which its output is shorted to ground. The quarter-wavelength line produces an open circuit at the opposite end where the outputs from multiple PAs are connected together to the load. This technique may be more easy to implement (especially for multiple PAs) than Doherty because a short is more readily realized than an open.

If PA #1 is the only PA active, its load is simply R_0. If both #1 and #2 are active, the combination produces an effective load impedance of 2Ro at the load ends of the lines. Inversion of this impedance through the lines places loads of $R_0/2$ on the RF PAs. Consequently, the peak power output for two active PAs is four times that with a single PA. As in discrete envelope tracking, the RF PAs operate as linear amplifiers. The number of PAs that are active is the minimum needed to produce the current output power. The peak power is thus kept relatively close to the saturated output, eliminating most of the effects of operating in back-off. The efficiency can therefore reach PEP efficiency at a number of different output levels, as shown in Figure 67.

The advantage of this technique is the ease in design associated with relying on short circuits rather than open circuits to isolate the off-state PAs. A possible disadvantage is operating individual PAs from multiple load impedances without retuning and a limited number of power steps available (e.g., 9/9, 4/9, 1/9 for a three-PA system).

Electronic Tuning

The performance of virtually all power amplifiers is degraded by load- impedance mismatch. Mismatched loads not only reduce efficiency, but also create higher stresses on the transistors. Because high-efficiency PAs generally require a specific set of harmonic impedances, their use is often restricted to narrow-band applications with well-defined loads.

Electronic tuning allows frequency agility, matching of unknown and variable loads, and amplitude modulation. Components for electronic tuning include pin-diode switches, MEMS switches, MEMS capacitors, semiconductor capacitors, ceramic capacitors (e.g., BST), and bias-controlled inductors. To date, electronic tuning has been applied mainly to small-signal circuits such as voltage-controlled oscillators. Recently demonstrated, however, are two electronically tuned power amplifiers. One operates in class E, produces 20 W with an efficiency of 60 to 70 percent, and can be tuned from 19 to 32 MHz (1.7:1 range) through the use of voltage-variable capacitors

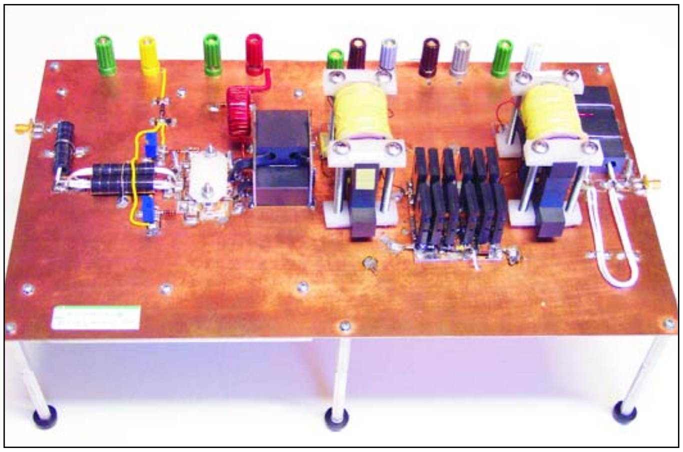

Figure 68 · Electronically tunable class-D PA (courtesy GMRR).

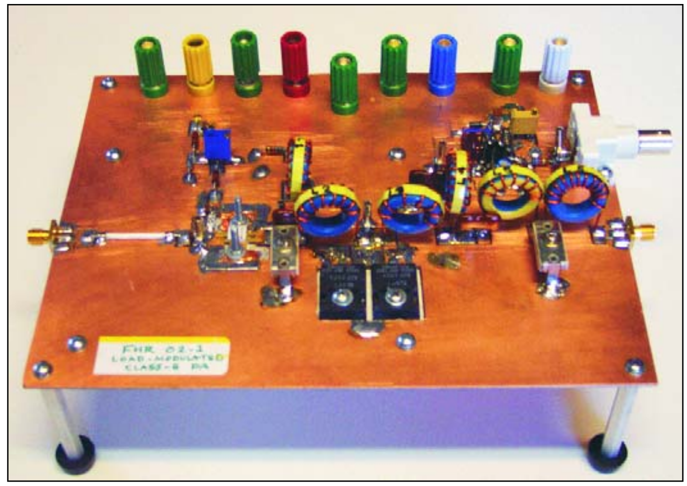

Figure 70 · Load-modulated class-E PA (courtesy GMRR).

[123, 124]. The second (Figure 68) operates in class D, produces 100 W with an efficiency of 60 to 70 percent, and can be tuned from 5 to 21 MHz (4.25:1 range) through the use of electronically tunable inductors and capacitors [125].

Load Modulation

The output of a power amplifier can be controlled by varying the drive, gate bias, DC supply voltage, or load impedance. "Load modulation" uses an electronically tuned output filter (Figure 69) to vary load impedance and thereby the instantaneous amplitude of the output signal. The modulation bandwidth can be quite wide, as it is limited only by the bias feeds to the tuning components.

A key aspect of load modulation is a diligent choice of the impedance locus so that it provides both good dynamic range and good efficiency. For ideal saturated PAs of classes A, B, C, and F, the optimum locus is the pure resistance line on the Smith chart that runs from the nominal load to an infinite load. For ideal class-E PAs with series inductance and shunt susceptance for optimum operation with the nominal load, the optimum locus is the unity-efficiency line running from the nominal load upward and rightward at an angle of 65° [126]. For real PAs, the optimum locus is found by examination of load-pull contours.

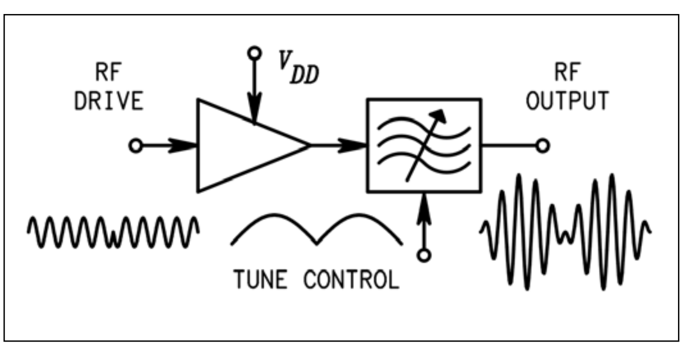

Figure 69 · Load modulation by electronic tuning.

The simple T filter has a single electronically variable element, but provides an approximately optimum locus for class E over the top 12 dB of the dynamic range. The experimental 20-W, 30-MHz [124, 126] shown in Figure 70 achieves a 41-dB range of amplitude variation. The measured instantaneous-efficiency curve (Figure 71) corresponds to a factor of 2.1 improvement in the average efficiency for a Rayleigh-envelope signal with a 10-dB peak-to-average ratio.

A load-modulated PA for communications follows the electronically tuned filter with a passive filter to remove the harmonics associated with the nonlinear elements. Predistortion compensates for the incidental phase modulation inherent in dynamic tuning of the filter. Variation of the drive level can be used to conserve drive power and to extend the dynamic range.

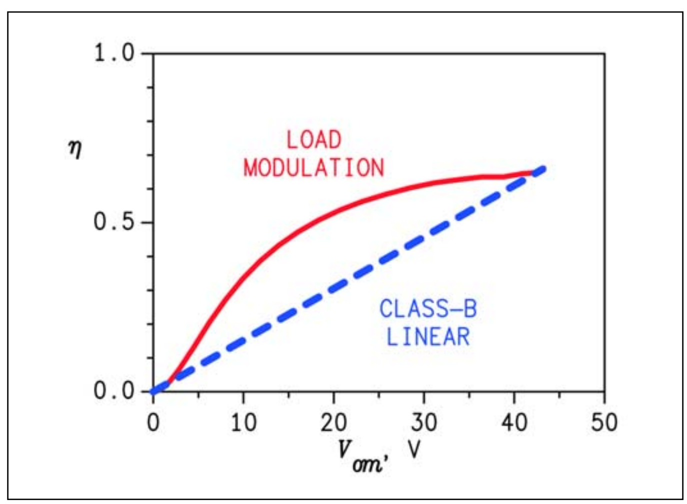

Figure 71 · Instantaneous efficiency of load modulation compared to class-B linear amplification.

References

112. Figures 8 and 9 in Part 2 of tis series, *High Frequency Electronics*, July 2003.

113. F. H. Raab, “Radio frequency pulsewidth modulation,” *IEEE Trans. Commun.*, vol. COM-21, no. 8, pp. 958-966, Aug. 1973.

114. F. G. Tinta, “Direct single sideband modulation of transmitter output switcher stages,” *Proc. RF Expo East ’86*, Boston, MA, pp. 313-398, Nov. 10-12, 1986.

115. A. Jayaraman, P. F. Chen, G. Hanington, L. Larson, and P. Asbeck, “Linear high-efficiency microwave power amplifiers using bandpass delta-sigma modulators,” *IEEE Microwave Guided Wave Lett.*, vol. 8, no. 3, pp. 121-123, March 1998.

116. J. Keyzer et al., “Generation of RF pulsewidth modulated microwave signals using delta-sigma modulation,” *2002 Int. Microwave Symp. Digest*, vol. 1, pp. 397-400, Seattle, WA, June 2-7, 2002.

117. J. D. Rogers and J. J. Wormser, “Solid-state high-power low frequency telemetry transmitters,” *Proc. NEC*, vol. 22, pp. 171-176, Oct. 1966.

118. R. E. Stengel and S. A. Olson, “Method and apparatus for efficient signal power amplification,” U.S. Patent 5,892,395, Apr. 6, 1999.

119. R. Langridge, T. Thornton, P. M. Asbeck, and L. E. Larson, “A power re-use technique for improving efficiency of outphasing microwave power amplifiers,” *IEEE Trans. Microwave Theory Tech.*, vol. 47, no. 8, pp. 1467-1470 , Aug. 1999.

120. S. Djukic, D. Maksimovic, and Z. Popovic, “A planar 4.5-GHz dc-dc power converter,” *IEEE Trans. Microwave Theory Tech.*, vol. 47, no. 8, pp. 1457-1460, Aug. 1999.

121. A. Shirvani, D. K. Su, and B. A. Wooley, “A CMOS RF power amplifier with parallel amplification for efficient power control,” *IEEE J. Solid- State Circuits*, vol. 37, no. 6, pp. 684-693, June 2002.

122. C. Y. Hang, Y. Wang, and T. Itoh, “A new amplifier power combining scheme with optimum efficiency under variable outputs,” *2002 Int. Microwave Symp. Digest*, vol. 2, pp. 913-916, Seattle, WA, June 2-7, 2002.

123. F. H. Raab, “Electronically tunable class-E power amplifier,” *Int. Microwave Symp. Digest*, Phoenix, AZ, pp. 1513-1516, May 20-25, 2001.

124. F. H. Raab, “Electronically tuned power amplifier,” Patent pending.

125. F. H. Raab and D. Ruppe, “Frequency-agile class-D power amplifier,” *Ninth Int. Conf. on HF Radio Systems and Techniques*, pp. 81-85, University of Bath, UK, June 23-26, 2003.

126. F. H. Raab, “High-efficiency linear amplification by dynamic load modulation,” *Int. Microwave Symp. Digest*, vol. 3, pp. 1717-1720, Philadelphia, PA, June 8-13, 2003.

Correction

In Part 4 of this series (Novermber 2003 issue), Figures 45, 52, 55, 56, 57 and 58 should have been credited as “Courtesy Andrew Corporation” instead of “Courtesy WSI.”

Author Information

The authors of this series of articles are: Frederick H. Raab (lead author), Green Mountain Radio Research, e-mail: f.raab@ieee.org; Peter Asbeck, University of California at San Diego; Steve Cripps, Hywave Associates; Peter B. Kenington, Andrew Corporation; Zoya B. Popovic, University of Colorado; Nick Pothecary, Consultant; John F. Sevic, California Eastern Laboratories; and Nathan O. Sokal, Design Automation. Readers desiring more information should contact the lead author.

Acronyms Used in Part 5

BST	Barium Strontium Titanate
GWEN	Ground Wave Emergency Network
PWM	Pulse-Width Modulation